

Online activity prediction via generalized Indian buffet process models

Mario Beraha¹, Lorenzo Masoero², Stefano Favaro^{3,4}, and Thomas S. Richardson^{2,5}

¹Department of Economics, Management, and Statistics, University of Milano–Bicocca

²Amazon, Inc.

³Department of Economics and Statistics, Università di Torino

⁴Collegio Carlo Alberto

⁵Department of Statistics, University of Washington

Abstract

Online A/B experiments generate millions of user-activity records each day, yet experimenters need timely forecasts to guide roll-outs and safeguard user experience. Motivated by the problem of activity prediction for A/B tests at Amazon, we introduce a Bayesian non-parametric model for predicting both first-time and repeat triggers in web experiments. The model is based on the stable beta-scaled process prior, which allows for capturing heavy-tailed behaviour without strict parametric assumptions. All posterior and predictive quantities are available in closed form, allowing for fast inference even on large-scale datasets. Simulation studies and a retrospective analysis of 1,774 production experiments show improved accuracy in forecasting new users and total triggers compared with state-of-the-art competitors, especially when only a few pilot days are observed. The framework enables shorter tests while preserving calibrated uncertainty estimates. Although motivated by Amazon’s experimentation platform, the method extends to other applications that require rapid, distribution-free prediction of sparse count processes.

Keywords: A/B testing, user prediction, Bayesian nonparametrics, scaled process priors, empirical Bayes.

1 Introduction

In the era of data-driven decision making, online A/B testing has emerged as a fundamental tool for evaluating the effectiveness of new interventions on key performance indicators in the technology industry (Kohavi et al., 2013; Gupta et al., 2019). By randomly assigning users to different versions of a product or service via an A/B test, experimenters can measure the causal impact of their interventions and make informed decisions about product development and user experience. The success of an online A/B test relies heavily on user engagement, which reflects the users' interest in and interaction with the product. Accurate prediction of user engagement, including the number of new users and their re-trigger rates, is crucial for planning and running efficient experiments.

Experimenters face a challenging trade-off when designing online A/B tests. On one hand, running shorter experiments can reduce costs and minimize the exposure of users to potentially suboptimal experiences. On the other hand, longer experiments can provide more representative data and improve the reliability of the results. Accurate predictions of user engagement can help experimenters navigate this trade-off and make informed decisions about the optimal experimental duration. By accurately forecasting the number of new users and their re-trigger rates, experimenters can ensure that they collect sufficient data to detect meaningful treatment effects while minimizing costs and risks associated with prolonged experimentation.

Existing methods for predicting user engagement in online A/B tests often make restrictive assumptions about user behavior, limiting their ability to capture the complex dynamics of user engagement over time. For example, some methods assume that the propensity to engage is equal for all users (both in the control and treatment group) (Deng, 2015) or model user-specific propensities as i.i.d. random variables (Richardson et al., 2022). Instead, in practice, one often observes a power-law behavior of users' activities, with few users being extremely active and most users seldom being active. Other methods require specifying an artificial upper bound on the total number of users (Richardson et al., 2022; Wan et al., 2023), which can be challenging to estimate and may lead to biased predictions. Moreover, many existing methods focus solely on predicting the number of new users, neglecting the important information contained in re-trigger rates, which can provide valuable insights into user loyalty and long-term engagement.

To overcome these limitations, we here propose a novel Bayesian nonparametric approach for predicting user engagement in online A/B tests. Our method leverages the stable beta-scaled process (SBSP) prior (Camerlenghi et al., 2022), a flexible and principled framework for modeling complex user propensity to (re)-triggering within an experiment. The SBSP prior allows for a rich representation of user heterogeneity while maintaining desirable properties. In particular, SBSP priors are analytically tractable, and produce closed-form expressions for many posterior quantities of interest. We consider two likelihood models: a Bernoulli model for daily user activity and a negative binomial model for re-trigger counts. For both models, we derive closed-form expressions for the posterior distribution and predictive quantities, enabling efficient inference and prediction without the need for computationally intensive sampling methods.

Through extensive simulations and real-world applications, we demonstrate the superior performance of our approach compared to existing methods. Our method consistently outperforms state-of-the-art alternatives in predicting both the number of new users and their re-trigger rates, achieving high accuracy even with limited pilot data. By accurately predicting user engagement, our approach can help experimenters plan and run more efficient experiments, reduce costs, and improve decision-making. Our contributions extend beyond the application of Bayesian nonparametric methods to online A/B testing, as the proposed methodology can be easily adapted to other domains where predicting user engagement is crucial, such as customer retention analysis and churn prediction.

The main contributions of this paper are threefold:

1. We introduce a flexible and principled Bayesian nonparametric framework for modeling user engagement in online A/B tests based on the stable beta-scaled process prior. Our approach allows for a rich representation of user heterogeneity and captures the complex dynamics of user engagement over time.
2. We derive closed-form expressions for the posterior distribution and predictive quantities for both the Bernoulli and negative binomial likelihood models. These analytical results enable efficient inference and prediction, making our approach well-suited for large-scale applications.
3. We demonstrate the superior performance of our approach through extensive simulations and real-world applications. Our method consistently outperforms state-of-the-art alternatives in predicting both the number of new users and their re-trigger rates, highlighting the practical value of Bayesian nonparametric methods in online A/B testing.

The rest of the paper is organized as follows. Section 2 describes the data and challenges of predicting user engagement in online A/B tests and reviews existing methods. Section 3 presents our Bayesian nonparametric methodology, including the stable beta-scaled process prior, likelihood models, and inference procedures. Section 4 discusses a practical numerical implementation of the derived methods. We report the experimental results on simulated results in section 5 and on real-world data in section 6, comparing our approach to state-of-the-art alternatives. Finally, section 7 discusses the implications of our findings, potential applications, and future research directions.

2 Data and Existing Methods

2.1 User Engagement Data in Online A/B Tests

In online A/B testing, users are randomly assigned to either the control or the treatment group. Each of these groups encodes a different version of the product or service that the experimenter is interested in testing. The goal is to measure the causal impact of the treatment on user behavior and key performance indicators (Kohavi et al., 2013). Within these tests, user engagement is a crucial component, as it reflects the users’ interest in and interaction with the product.

We consider data from online A/B tests consisting of daily user activity over a fixed time period. For each user n , we observe the day of their first trigger in the experiment $F_n \in \mathbb{N}$ (i.e., the time and day they first engage with the product) and, possibly, the count $A_{d,n} \geq 0$ of their subsequent re-triggers for each day d . In certain settings, where the service running the experiment only records coarse activity data, $A_{d,n}$ might simply be a binary indicator of whether user n engaged on day d . It follows by construction that $F_n = \min_d I[A_{d,n} > 0]$, where $I[\cdot]$ denotes the indicator function. The data can be represented as a set of tuples $\{(\omega_n, F_n, A_{1:D,n})\}_{n=1}^N$, where ω_n is a unique identifier for user n , D is the total number of days in the experiment, and N is the total number of users who engaged with the product during the experiment. We here use the shorthand notation $X_{a:b} := X_a, X_{a+1}, \dots, X_b$.

One of the main challenges in modeling user engagement data is its sparsity and heterogeneity. In typical online A/B tests, a large proportion of users may engage with the product only once or a few times, while a small fraction of users may exhibit high levels of engagement. Moreover, users may have different propensities to engage with the product over time, leading to complex dynamics in the re-trigger counts. Capturing this heterogeneity and temporal dependence is crucial for accurately predicting user engagement.

2.2 Existing methods for predicting user engagement

Several methods have been proposed to predict user engagement in online A/B tests and related settings. We here consider the problem of predicting the number of users that did not trigger in the first D_0 days (the *pilot* study) but will trigger in days $D_0 + 1, \dots, D_0 + D_1$ (the *follow-up* period), and cast it as an *unseen feature problem*. Formally, the goal of the analysis is to estimate

$$U_{D_0}^{(D_1)} := \sum_{n \geq 1} I \left\{ \left[\sum_{d=1}^{D_0} A_{d,n} = 0 \right] \cap \left[\sum_{d=1}^{D_0} A_{d,n} > 0 \right] \right\}, \quad (1)$$

where the outer sum ranges over all possible users.

We can broadly categorize methods to estimate $U_{D_0}^{(D_1)}$ into statistical and algorithmic approaches. In recent years, many interesting approaches have been developed in the context of genomic studies. In the former category, [Gravel \(2014\)](#) employed jackknife estimators based on the first few values of the resampling frequency spectrum. More recently, [Chakraborty et al. \(2019\)](#) proposed to use the celebrated Good-Toulmin estimator ([Good, 1953](#)) to predict the number of new genomic variants based on the observed frequency counts. [Richardson et al. \(2022\)](#) focused on user engagement prediction and proposed a Bayesian model for the first trigger times. Other Bayesian approaches to the unseen feature problem can be found in [Ionita-Laza et al. \(2009\)](#); [Masoero et al. \(2022\)](#); [Camerlenghi et al. \(2022\)](#). By contrast, [Zou et al. \(2016\)](#) proposed to solve the unseen feature problem via a linear programming approach.

This paper focuses on statistical approaches to the unseen feature problem and its generalizations. In particular, we take a Bayesian model-based approach for two reasons. First, our data consists of only a handful of experiment days (namely $D_0 \leq 7$). Bayesian methods are well-suited for settings where predictions have to be formed with limited amounts of input “training” data, thanks to the possibility of eliciting informative prior information that regularizes the inference. Moreover, our goal is not user prediction per se but rather to inform online experiments that must decide the duration of A/B tests and whether a specific experiment should be terminated immediately after observing the first D_0 days. Therefore, providing experimenters with probabilistic predictions and credible intervals helps them make more informed decisions.

The previously proposed Bayesian approaches to the unseen feature problems exhibit distinct drawbacks when applied to user engagement data. [Ionita-Laza et al. \(2009\)](#); [Richardson et al. \(2022\)](#) assume that the total number of users, say M , is fixed and known. Beyond the obvious difficulty of picking such a parameter from the available data, this assumption clearly implies $U_{D_0}^{(D_1)} \rightarrow M - N_{D_0}$ almost surely as $D_1 \rightarrow \infty$, where N_{D_0} is the number of users that triggered in the first D_0 days. In contrast, user activity often exhibits a power law growth, i.e., $U_{D_0}^{(D_1)} \sim D_1^\gamma$

for some $\gamma \in (0, 1)$. [Masoero et al. \(2022\)](#); [Camerlenghi et al. \(2022\)](#) assume two different Bayesian nonparametric models, both based on a generalization of the celebrated Indian buffet process ([Griffiths and Ghahramani, 2011](#)). In their framework, the total number of users is unbounded, but the number of users that trigger in any finite timeframe is finite, almost surely. Moreover, both models exhibit a power law growth for the number of users. A limitation of both models is that they can only be applied to coarse activity data, i.e., when $A_{d,n}$ is a binary indicator of whether user n is active on day d . This implies losing information when using granular daily activity data. Moreover, in some situations, focusing only on the first trigger times F_n might be preferable as we demonstrate in our experiments. Hence, there is currently a lack of flexibility that affects modeling choices when employing a Bayesian nonparametric approach.

3 Bayesian Nonparametric Methodology

This section presents our Bayesian approach for predicting user engagement in online A/B tests. We first set up a general framework encompassing all previously proposed Bayesian models as special cases. We highlight how the choice the prior distribution plays a crucial role for the quality of the posterior and predictive distributions of interest. We then discuss using a stable beta-scaled process prior and show how this results in a flexible model that retains analytical tractability and closed-form expressions for posterior inferences. We frame our model within the class of Bayesian trait processes ([James, 2017](#); [Campbell et al., 2018](#); [Masoero et al., 2018](#); [Beraha and Favaro, 2023](#)).

3.1 Trait process formulation

We first recall the definition of a trait process ([Campbell et al., 2018](#); [James, 2017](#)).

Definition 3.1 (Trait Process). *Let $\mu = \sum_{n \geq 1} \theta_n \delta_{\omega_n}$ be an almost surely discrete random measure with distribution \mathcal{P}_μ , where δ_x is the Dirac delta at x . Given μ , let $Z_d = \sum_{n \geq 1} A_{d,n} \delta_{\omega_n}$, $d \geq 1$ such that for a score distribution \mathcal{G} with support on \mathbb{N} ,*

$$A_{d,n} \mid \mu \stackrel{iid}{\sim} \mathcal{G}(\cdot \mid \theta_n),$$

and $A_{d,n} \perp A_{d',n'} \mid \mu$ for any d, d', n, n' with $(d, n) \neq (d', n')$. Then we say that $(Z_d)_{d \geq 1}$ is a trait process directed by μ with score distribution \mathcal{G} . Compactly, we write

$$Z_d \mid \mu \stackrel{iid}{\sim} \text{TrP}(\mu, \mathcal{G}), \quad \mu \sim \mathcal{P}_\mu. \quad (2)$$

To connect the framework of definition 3.1 with our data discussed in section 2, we represent observations as a discrete measure supported over the user identifiers. Specifically, we view data collected during day d of the experiments as

$$Z_d(\cdot) = \sum_{n \geq 1} A_{d,n} \delta_{\omega_n}(\cdot), \quad d = 1, \dots, D. \quad (3)$$

From the definition above, the relation $Z_d(\omega_n) = A_{d,n}$ gives a way of pairing each daily activity index $A_{d,n}$ of the n -th unit on the d -th day together with the label ω_n of the n -th unit.

Similarly, let

$$Z^{\text{FT}}(\cdot) = \sum_{n \geq 1} F_n \delta_{\omega_n}(\cdot), \quad (4)$$

which is a measure that collects only the first triggering time (FT) of all active users. Here, we let both measures Z_d and Z^{FT} range over an infinite sum by letting $A_{d,n} = 0$ for any user n that did not trigger on day d and $F_n = 0$ for all users that did not trigger in the first D days.

We assume that Z_d 's in eq. (3) follow a trait process with score distribution defined as follows. When the data consists of daily indicator variables for each user, then $\mathcal{G} = \mathcal{G}_{\text{Be}}$ is the Bernoulli distribution with success probability θ — every $A_{d,n} | \mu \sim G_{\text{Be}}(\theta_n)$ independently across n and i.i.d. across d for the same n . If, instead, we have daily re-trigger data for each user ($A_{d,n} \in \mathbb{N}$), we let $\mathcal{G} = \mathcal{G}_{\text{NB}}$ be the negative binomial distribution with parameters $(r, 1 - \theta)$ — every $A_{d,n} | \mu \sim G_{\text{NB}}(r, 1 - \theta_n)$ independently across n and i.i.d. across d for the same n . Parametrizing the success probability of the negative binomial distribution with $(1 - \theta)$ is needed since for the class of priors \mathcal{P}_μ under consideration here, the distribution of θ_n concentrates on infinitesimally small values. With our choice of parametrization, this means that for any given experimental duration, only a finite number of users will be active, see [Beraha and Favaro \(2023\)](#) for a proof. Similarly, we assume a trait process for (4) where $\mathcal{G} = \mathcal{G}_{\text{TG}}$ is the probability mass function over $\{0, 1, \dots, D\}$ given by

$$\mathcal{G}_{\text{TG}}(y; \theta) = \begin{cases} (1 - \theta)^{y-1} s & \text{if } 1 \leq y \leq D, \\ 1 - (1 - \theta)^D & \text{if } y = 0, \end{cases} \quad (5)$$

i.e. \mathcal{G}_{TG} is a *truncated* geometric distribution which puts to zero all values greater than D .

All the previously proposed Bayesian methodologies for the unseen feature problem (cf. section 2.2) can be recovered as special cases of this trait process framework. In particular, the model in [Masoero et al. \(2022\)](#) is equivalent to eq. (3) where $\mathcal{G} = \mathcal{G}_{\text{Be}}$ and \mathcal{P}_μ is the law of the (three-parameter) beta process ([Teh and Gorur, 2009](#); [Broderick et al., 2012](#)). Similarly,

the beta-binomial model of Ionita-Laza et al. (2009) is recovered from (3) when $\mathcal{G} = \mathcal{G}_{\text{Be}}$ and $\mu = \sum_{n=1}^N \theta_n \delta_{\omega_n}$ where N is the total number of users (assumed fixed) and $\theta_n \stackrel{\text{iid}}{\sim} \text{Beta}(a, b)$. Finally, the hierarchical beta-geometric model of Richardson et al. (2022) is recovered from eq. (4) choosing \mathcal{G}_{TG} and assuming the same prior for μ as in the beta-binomial model. Hence, while the likelihood models described above can accommodate various types of user engagement data, the choice of the prior distribution for μ is crucial for capturing the complex dynamics and heterogeneity of user behavior. Previously proposed Bayesian methods make restrictive assumptions about the form of μ , limiting their ability to model sparse and diverse user engagement patterns. To address these limitations, we propose using the stable beta-scaled process (SBSP) prior (Camerlenghi et al., 2022) for μ .

3.2 Stable Beta-Scaled Process Prior

The SBSP prior is a flexible and tractable prior distribution that allows for a rich representation of user heterogeneity while maintaining desirable properties such as exchangeability and analytical tractability. To define it, consider an α -stable random measure $\mu = \sum_{n \geq 1} \tau_n \delta_{\omega_n}$. That is, μ is a CRM with Lévy intensity $\alpha s^{-1-\alpha} ds P_0(dx)$ for $0 < \alpha < 1$. Denote by $\Delta_1 > \Delta_2 > \dots$ the decreasingly ordered random jumps τ_n of μ . Following Ferguson and Klass (1972) Δ_1 has density $f_{\Delta_1}(\zeta) = \exp\{\alpha \int_{\zeta}^{+\infty} s^{-1-\alpha} ds\} \alpha \zeta^{-1-\alpha}$, i.e., $\Delta_1^{-\alpha} \sim \mathcal{E}(1)$. Denote by $\mathcal{L}_{\zeta}(\cdot)$ the conditional distribution of $(\Delta_{n+1}/\Delta_1)_{n \geq 1}$ given $\Delta_1 = \zeta$. Then, a scaled process is obtained by marginalizing Δ_1 from the latter distribution. As noted in James et al. (2015), we can gain in flexibility by changing the law of Δ_1 , i.e., marginalizing $\mathcal{L}_{\zeta}(\cdot)$ with respect to $\zeta \sim h^*$ for any distribution h^* supported on the non-negative reals. The stable beta-scaled process is obtained by a suitable choice of h^* .

Definition 3.2. *A stable beta-scaled process (SB-SP) prior is the law of random measure $\mu = \sum_{n \geq 1} \theta_n \delta_{\omega_n}$ where $\omega_n \stackrel{\text{iid}}{\sim} P_0$ and $(\theta_n)_{n \geq 1}$ is distributed as $\int \mathcal{L}_{\zeta}(\cdot) h_{\alpha, c, \beta}(\zeta) d\zeta$ where*

$$h_{\alpha, c, \beta}(\zeta) = \Gamma(c+1)^{-1} \alpha \beta^{c+1} \zeta^{-\alpha(c+1)-1} \exp\{-\beta \zeta^{-\alpha}\},$$

for $0 < \alpha < 1$, $\beta > 0$, and $c > 0$. We will use the notation $\tilde{\mu} \sim \text{SB-SP}(\alpha, c, \beta)$.

We introduce the following notation for shorthand convenience.

Definition 3.3. *Let $\mu \sim \text{SB-SP}(\alpha, c, \beta)$. If Z_d is as in eq. (3), $Z_d \mid \mu \stackrel{\text{iid}}{\sim} \text{TrP}(\mathcal{G}_{\text{NB}}; \mu)$, we say that $Z_{1:D} = (Z_1, \dots, Z_D)$ follows a negative binomial stable beta scaled process and write $Z_1, \dots, Z_D \sim \text{NB-SSP}$. If, instead, $\mathcal{G} = \mathcal{G}_{\text{Be}}$, we say that $Z_{1:D}$ follows a Bernoulli stable*

beta scaled process and write $Z_1, \dots, Z_D \sim \text{Be-SSP}$. Finally, if Z^{FT} is as in (4), such that $Z^{\text{FT}} | \mu \sim \text{TrP}(\mathcal{G}_{\text{TG}}; \mu)$ where \mathcal{G}_{TG} is as in (5), we say that Z^* follows a truncated geometric stable beta scaled process and write $Z^{\text{FT}} \sim \text{TG-SSP}$.

3.3 Posterior Distribution and Predictive Quantities

Central to obtaining computationally feasible estimators for the future user engagement is the study of the posterior and predictive distributions under the trait process model. By extending the Poisson partition calculus developed in [James \(2017\)](#) for CRM priors, the next theorem gives a unified template for the posterior distribution under the SB-SP priors.

We introduce some additional notation. For a sample $Z_{1:D}$ from (2), let $\omega_{1:N_D}^*$ be the N_D unique feature labels displayed in such a sample (i.e., in our notation, the unique user identifiers of those active users). For $n = 1, \dots, N_D$ define the index set $\mathcal{B}_n = \{i \in \{1, \dots, D\} : Z_d(\omega_n^*) > 0\}$; i.e., \mathcal{B}_n collects the days in which user ω_n^* was active. Let $m_n = |\mathcal{B}_n|$ be its cardinality (i.e., the count of the days during which user n was active).

Theorem 3.4. *Let $Z_{1:D}$ be a sample from (2), where $\mu \sim SB-SP(\alpha, c, \beta)$. Then, the posterior distribution of μ given $Z_{1:D}$ coincides with the law of*

$$\sum_{n=1}^{N_D} \theta_n^* \delta_{\omega_n^*} + \mu'$$

such that

1. $(\theta_n^*)_n \geq 1$ are independent random variables with marginal density

$$f_{\theta_n^*}(\theta) \propto (1 - \pi_{\mathcal{G}}(\theta))^{D-m_n} \theta^{-1-\alpha} \prod_{d \in \mathcal{B}_n} \mathcal{G}(A_{d,n}; \theta) \quad (6)$$

2. μ' is a random measure independent of the θ_n^* 's with law

$$\begin{aligned} \mu' | \tilde{\Delta}_{1,h} &\sim \text{CRM} \left(\tilde{\Delta}_{1,h}^{-\alpha} (1 - \pi_{\mathcal{G}}(\theta))^D s^{-1-\alpha} ds P_0(d\omega) \right) \\ \tilde{\Delta}_{1,h}^{-\alpha} &\sim \text{Gamma} \left(N_D + c + 1, \beta + \alpha \int_0^1 (1 - (1 - \pi_{\mathcal{G}}(\theta))^D) \theta^{-1-\alpha} d\theta \right) \end{aligned} \quad (7)$$

From theorem 3.4 it is straightforward to obtain a formal description of the predictive distribution for $Z_{D+1} | Z_1, \dots, Z_D$. Indeed, we have

$$Z_{D+1} | Z_1, \dots, Z_D = \sum_{n=1}^{N_D} Z_{D+1,n}^* \delta_{\omega_n^*} + Z'_{D+1}, \quad (8)$$

where $Z_{D+1,n}^* | \theta_n^* \sim \mathcal{G}(\cdot; \theta_n^*)$ and $Z' | \mu' \sim \text{TrP}(\mu'; \mathcal{G})$ for θ_n^* and μ' as in Theorem 3.4.

To specialize theorem 3.4 to the three models under consideration, we observe the following. If data is as in (3), the sample size D corresponds to the number of days D_0 ; instead, if data is as in (4), the sample size is equal to one. In both cases, the number of unique features N_D in the sample is the number of users that were active in the pilot study (i.e., the first D_0 days), namely N_{D_0} .

Then, we obtain the following expressions for the posterior distributions under the three models considered.

Corollary 3.5. *Let $B(a, b) = \Gamma(a)\Gamma(b)/\Gamma(a+b)$ be the beta function. For $x, y, r > 0$, let*

$$\psi_r(x, y) = \alpha [B(rx + 1, -\alpha) - B(r(x+y) + 1, -\alpha)].$$

Then for all the BNP models considered — NB-SSP, Be-SSP, or TG-SSP — the posterior of μ is equivalent to the law of

$$\sum_{n=1}^{N_{D_0}} \theta_n^* \delta_{\omega_n^*} + \mu', \quad \mu' = \sum_{\ell \geq 1} \theta'_\ell \delta_{\omega'_\ell}. \quad (9)$$

In particular, μ' collects all the user-specific parameters θ'_ℓ of those users ω'_ℓ that did not trigger in the first N_{D_0} days. Moreover, $\tilde{\Delta}_{1,h}^{-\alpha} \sim \text{Gamma}(N_D + c + 1, \beta + \psi_r(0, D))$ with $r = 1$ under the Be-SSP and TG-SSP models, while $\theta_n^ \stackrel{\text{ind}}{\sim} \text{Beta}(a_n, b_n)$ with*

$$(a_n, b_n) = \begin{cases} (m_n - \alpha, rD + 1) & \text{under the NB-SSP model} \\ (m_n - \alpha, D - m_n + 1) & \text{under the Be-SSP model} \\ (1 - \alpha, F_n) & \text{under the TG-SSP model} \end{cases}$$

Notice that, rather surprisingly, the posterior for μ' coincides for the Be-SSP and TG-SSP models. This entails that the predictive distribution of quantities that can be expressed as functionals of μ' will be the same under Be-SSP and TG-SSP models. As a prominent example, we consider next the distribution of the number of new users that were not active in the first D_0 days but are active at least once in the following D_1 days.

Proposition 3.6. *Let N_d^* be the number of users that trigger for the first time on the d -th day ($d > D_0$). Then, conditionally on $\tilde{\Delta}_{1,h}$ as in corollary 3.5, $N_d^* \sim \text{Poi}(\alpha \tilde{\Delta}_{1,h}^{-\alpha} B(1 - \alpha, d))$. Let $U_{D_0}^{(D_1)} = \sum_{d=D_0}^{D_1} N_d^*$ be the number of users that were not active in the first D_0 days but are*

active at least once between days $D_0 + 1, \dots, D_0 + D_1$ as per eq. (1). Then under all the three models, the posterior distribution of $U_{D_0}^{(D_1)}$ given the data is

$$U_{D_0}^{(D_1)} \sim \text{NegBin} \left\{ N_{D_0} + c + 1, p_{D_0}^{(D_1)} \right\},$$

where

$$p_{D_0}^{(D_1)} = \frac{\psi_r(D_0, D_1)}{\beta + \psi_r(0, D_0 + D_1)}$$

with $r = 1$ for the Be-SSP and TG-SSP models.

Using proposition 3.6, we obtain a point estimator for the number of new users that will trigger in the following D_1 days by taking the expectation of $U_{D_0}^{(D_1)}$, which reduces to

$$\hat{U}_{D_0}^{(D_1)} = (N_{D_0} + c + 1) \frac{p_{D_0}^{(D_1)}}{1 - p_{D_0}^{(D_1)}}. \quad (10)$$

In addition to estimating the number of new users that will be active at least once in a follow-up observation period, another quantity of interest to experimenters is the number of total future re-trigger rates. Assuming that data is as in eq. (3) where $A_{d,n}$ denotes the number of triggers of the n -th user on day d , then the total number of triggers in the follow-up period of D_1 days is defined as $T_{D_0}^{(D_1)} = \sum_{d=1}^{D_1} \sum_{n \geq 0} A_{d+D_0, n}$. This information can be estimated using the NB-SSP model.

To this end, denote by $U_{D_0}^{(D_1,j)}$ be the number of users who have not triggered before day D_0 and will trigger exactly $j \geq 1$ times in a follow-up period of D_1 days. Namely,

$$U_{D_0}^{(D_1,j)} = \sum_{n \geq 1} \mathbb{I} \left[\sum_{d=1}^{D_0} A_{d,n} = 0 \right] \mathbb{I} \left[\sum_{d=1}^{D_1} A_{D_0+d,n} = j \right].$$

Similarly, denote by $S_{D_0}^{(D_1)}$ be the total re-triggers caused by the previously observed N_{D_0} users in the follow-up period, that is:

$$S_{D_0}^{(D_1)} = \sum_{d=1}^{D_1} \sum_{n=1}^{N_{D_0}} A_{D_0+d,n}.$$

The following proposition characterizes the distribution of re-trigger rates.

Proposition 3.7. *Let $Z_{1:D} \sim \text{NB-SSP}$. Then the posterior of $T_{D_0}^{(D_1)}$ given $Z_{1:D}$ coincides with the law of $\sum_{j \geq 1} j U_{D_0}^{(D_1,j)} + S_{D_0}^{(D_1)}$, such that*

$$U_{D_0}^{(D_1,j)} \mid Z_{1:D_0} \sim \text{NegBin}(N_{D_0} + c + 1, p_{D_0}^{(D_1,j)}),$$

with

$$p_{D_0}^{(D_1,j)} = \frac{\rho_{D_0}^{(D_1,j)}}{\beta + \psi_r(D_0, 0)}, \quad \rho_{D_0}^{(D_1,j)} = \binom{j + rD_1 + 1}{j} \alpha B(r(D_0 + D_1) + 1, j - \alpha).$$

Moreover,

$$S_{D_0}^{(D_1)} | Z_{1:D_0} = \sum_{n=1}^{N_{D_0}} \text{NegBin}(rD_1, \theta_n^*)$$

where $\theta_n^* \sim \text{Beta}(m_n - \alpha, rD_0 + 1)$ is as in item 1. of Corollary 3.5.

The Bayesian estimator for $T_{D_0}^{(D_1)}$ is then

$$\hat{T}_{D_0}^{(D_1)} = \mathbb{E} \left[T_{D_0}^{(D_1)} | Z_{1:D_0} \right] = (N_{D_0} + c + 1) \left[\sum_{j \geq 1} j \frac{p_{D_0}^{(D_1,j)}}{1 - p_{D_0}^{(D_1,j)}} \right] + \frac{D_1}{D_0} (T_0^{D_0} - N_{D_0} \alpha),$$

where $T_0^{(D_0)}$ is the total number of observed triggers in the first D_0 days.

3.4 Estimating the number of days to reach a participation threshold

We consider now a related but slightly different prediction problem: suppose that we would like for the A/B test to reach a target level of traffic, so that $N_{D_0} + M$ users are exposed to the intervention before it is terminated. We will now show how our models can be used to estimate the number of days needed to reach this inclusion level, based on pilot data.

Let D_M be the number of follow-up days needed to see M new users. The posterior of D_M can be determined as follows. Let $F' = \sum_{\ell \geq 1} F'_\ell \delta_{\omega'_\ell}$ denote the measure tracking the first triggering time of all the unobserved users and denote by $F'_{(\ell)}$ the ℓ -th smallest weight of F' . Then $D_M = F'_{(M-N_{D_0})}$. Unfortunately, the direct study of $F'_{(M-N_{D_0})}$ is prohibitive: it can be proved that this quantity is an order statistics of a mixed Poisson process with non-constant rate, for which no closed form expression exists. Nonetheless, we can simulate from D_M and approximate its posterior via Monte Carlo.

Simulating directly from F' is cumbersome since it involves countably many random variables. Therefore, we define a suitable upper bound D^{up} for D_M and simulate the first triggering time for those users that trigger before D^{up} . The next theorem provides the key technical ingredient for this strategy. For integers $a < b$ and $p \in (0, 1)$, denote by $\text{TGeom}(\cdot; p, a, b)$ the following truncated geometric probability mass function

$$\text{TGeom}(y; p, a, b) = \begin{cases} (1 - p)^{y-a} p & \text{if } a \leq y \leq b, \\ 1 - (1 - p)^{b-a+1} & \text{if } y = 0. \end{cases}$$

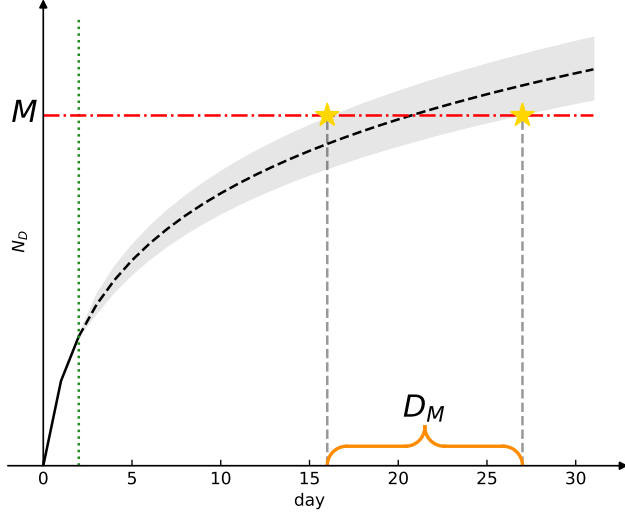


Figure 1: Inversion technique to estimate D_M . The solid black line represent the data. Dashed black line and gray area are the mean and the global credible band of $N_{D_0} + U_{D_0}^{(\ell)}$, where ℓ varies across the horizontal axis. The interval for D_M (orange curly bracket) is obtained by slicing the grey area at M .

Theorem 3.8. Let F' be defined as above and let $\tilde{F} = \sum_{\ell \geq 1} F'_\ell \mathbf{1}\{F'_\ell \leq D^{up}\} \delta_{\omega'_\ell}$. Then, conditionally to μ as in (9), \tilde{F} is distributed as a trait process directed by $\mu' = \sum_{\ell \geq 1} \theta'_\ell \delta_{\omega'_\ell}$ with score distribution $\theta'_\ell \mapsto \text{TGeom}(\cdot; \theta'_\ell, D_0, D^{up})$ for the Be-SSP and TG-SSP models and score distribution $\theta'_\ell \mapsto \text{TGeom}(\cdot; 1 - (1 - \theta'_\ell)^r, D_0, D^{up})$ for the NB-SSP model.

Moreover, marginalizing out μ' we have

$$\tilde{F} \stackrel{d}{=} \sum_{\ell=1}^{\xi} \tilde{F}'_\ell \delta_{\omega'_\ell},$$

where

$$\xi \sim \text{NegBin} \left(N + c + 1, 1 - \frac{\psi_r(D^{up}, D_0)}{\beta + \psi_r(D_0 + D^{up}, 0)} \right),$$

$\omega'_\ell \stackrel{iid}{\sim} P_0$ and \tilde{F}'_ℓ are i.i.d. random variables supported on $\{d + 1, \dots, d + D^{up}\}$ such that $\Pr(Y'_\ell = y) \propto B(1 - \alpha, y)$.

Building on the characterization in Theorem 3.8, we can simulate from the posterior of D_M using Algorithm 1. Algorithm 1 provides exact samples from the posterior of D_M , i.e., it does not require a burn-in period like Markov chain Monte Carlo.

While sampling from the exact distribution of interest, algorithm 1 can require a large number of samples to provide reliable estimates and can therefore be computationally expensive, especially in settings when N_{D_0} is large, say in the order of the hundreds of thousands or larger. Therefore, for those situations, we propose an alternative heuristic method based on ‘‘slicing’’ a

Algorithm 1 Posterior sampling for D_M

Input: Observations, number of Monte Carlo iterations K .

for $k = 1, \dots, K$ **do**

 Sample \tilde{F} using the representation of Theorem 3.8.

 Let $\tilde{F}'_{(\ell)}$ be sorted the jumps \tilde{F}'_ℓ .

 Set $D_k = \tilde{F}'_{(M-N_D)}$.

end for

Return: D_1, \dots, D_K .

global prediction band for the trajectory of the number of users that trigger before day ℓ , i.e., $N_{D_0} + U_{D_0}^{(\ell)} =: N_{D_0+\ell}$, as depicted in fig. 1.

To construct a global credible band for $(N_{D_0+\ell})_{\ell \geq 1}$, we work with the random variables N_d^* introduced in proposition 3.6. Indeed, for any ℓ , $(N_{D_0+1}, \dots, N_{D_0+\ell})$ and (N_1^*, \dots, N_ℓ^*) are in one-to-one correspondence given the observed data. In particular, we aim at constructing a global credible band, of level ε , of the form $\{(n_{D_0+\ell}^{lo}, n_{D_0+\ell}^{hi})\}_{\ell=1}^{D^{up}}$ such that $\Pr(n_{D_0+\ell}^{lo} \leq N_{D_0+\ell} \leq n_{D_0+\ell}^{hi} \text{ for all } \ell | Z_{1:D_0}) \geq 1 - \varepsilon$. First we simulate Q times from the posterior law of $\tilde{\Delta}_{1,h}$ as in Corollary 3.5 and, conditional on $\tilde{\Delta}_{1,h}$, we sample the values N_ℓ^* , $\ell = 1, \dots, D^{up}$ as in Proposition 3.6, keeping only the $(1 - \varepsilon)Q$ tuples of $(\tilde{\Delta}_{1,h}, \{N_\ell^*\}_{\ell=1}^{D^{up}})$ with highest posterior density. Then, we evaluate the $(1 - \varepsilon)Q$ trajectories for $N_{D_0+\ell} = N_{D_0} + \sum_{j \leq \ell} N_j^*$, denoted by $\{(N_{D_0+1}^{(k)}, \dots, N_{D_0+D^{up}}^{(k)}), k = 1, \dots, (1 - \varepsilon)Q\}$ and set

$$n_{D_0+\ell}^{lo} = \min_k N_{D_0+\ell}, \quad n_{D_0+\ell}^{hi} = \max_k N_{D_0+\ell}.$$

We found that the interval for D_M is robust to the chosen value of D^{up} if this is sufficiently large. We always fix $D^{up} = 3\mathring{D}_M$ in our simulations, where \mathring{D}_M is a point estimate for D_M defined by $N_{D_0} + \hat{U}_{D_0}^{(D_M)} \approx M$.

4 Numerical Implementation

The theoretical results derived in Section 3 yield close form expression for Bayesian point estimators, in the form of posterior expectations of functionals of interest, as well as uncertainty quantification, in the form of credible intervals. Crucially, the expressions found depend on key parameters (α, c, β) in the case of Be-SP-SP and TG-SSP models and (α, c, β, r) for the NB-SSP model.

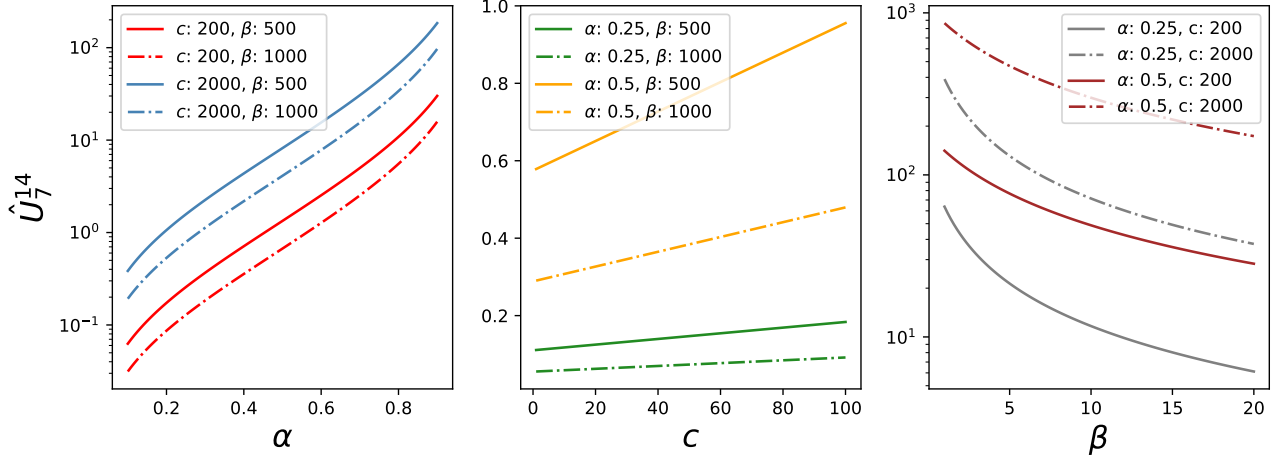


Figure 2: Values of $\hat{U}_7^{(14)}$ for different choices of parameters (α, c, β) and $r = 1$

Inspecting, for instance, the expectation of $U_{D_0}^{(D_1)}$ in eq. (10) sheds light on the role played by the different parameters, cf. fig. 2. However, it is clear that there is a strong interplay between such parameters, making prior elicitation hard. For instance, $U_{D_0}^{(D_1)}$ is an increasing function of α and c a decreasing function of β . Moreover, prior elicitation must be carried out experiment-by-experiment, which is time-consuming and infeasible in large-scale applications of A/B tests, where thousands of tests are performed daily. Hence, we take an empirical Bayesian approach and estimate such parameters from the available data. Compared to being “fully Bayesian”, i.e., assuming prior distributions for such hyperparameters, our strategy is more scalable as it does not require performing Markov chain Monte Carlo simulations.

4.1 Parameter estimation by maximum marginal likelihood

A natural option to estimate unknown parameters involved in the likelihood and prior distributions is maximizing the observed data’s marginal likelihood. See, e.g., [Carlin and Louis \(2000\)](#). To this end, the next result gives an explicit expression for the marginal distribution of the data.

Theorem 4.1. *Let Z_1, \dots, Z_{D_0} be a sample under either the NB-SSP, Be-SSP, or TG-SSP model, such that N_{D_0} unique users with labels $\omega_1^*, \dots, \omega_{N_{D_0}}^*$ were active. For the NB-SSP and Be-SSP models, let $m_n = \sum_{d=1}^{D_0} A_{d,n}$ be the total activity count for unit n in the first D_0 days. Then, the joint distribution of Z_1, \dots, Z_{D_0} , when the distributions of the user labels are marginalized out, is*

$$\Pr(Z_1, \dots, Z_{D_0}) = \frac{\alpha^{N_{D_0}} \beta^{c+1}}{(\beta + \psi(0, D_0, r))^{N_{D_0}+c+1}} \frac{\Gamma(N_{D_0} + c + 1)}{\Gamma(c)} \prod_{n=1}^{N_{D_0}} \Theta_n \quad (11)$$

where $r = 1$ for the Be-SSP and TG-SSP models and

$$\Theta_n = \begin{cases} \prod_{d:A_{d,n}>0} \binom{A_{d,n}+r-1}{A_{d,n}} B(rD_0+1, m_n - \alpha + 1) & \text{under the NB-SSP model} \\ B(m_n - \alpha, D_0 - m_n + 1) & \text{under the Be-SSP model} \\ B(1 - \alpha, F_n) & \text{under the TG-SSP model} \end{cases}$$

Defining the marginal likelihood for parameters α, c, β , and possibly r , as $\mathcal{L}(\alpha, c, \beta, r) = \Pr(Z_1, \dots, Z_{D_0}; \alpha, c, \beta, r)$, the empirical Bayesian strategy is to set such parameters as

$$\hat{\alpha}, \hat{c}, \hat{\beta}, \hat{r} = \arg \max_{\alpha, c, \beta, r} \log \mathcal{L}(\alpha, c, \beta, r). \quad (12)$$

The optimization problem is nonconvex in its variables. Therefore, we adopt the `scipy` implementation of the differential evolution algorithm (Storn and Price, 1997), which is a derivative-free global optimization algorithm.

4.2 Parameter estimation by curve fitting

Another option is to frame parameter elicitation as a curve fitting problem for the temporal trajectory of a statistic of interest. For example, we might want to predict the number of future users first triggering in the next D_1 days, using the point estimator of Equation (10). We fit the hyperparameters by solving the following regression problem:

$$\hat{\alpha}, \hat{c}, \hat{\beta}, \hat{r} = \arg \min_{\alpha, c, \beta, r} \sum_{d=1}^{D_0-d_0} \left\{ \hat{U}_{d_0}^{(d)} - u_{d_0}^{(d)} \right\}^2, \quad (13)$$

where $u_{d_0}^{(d)}$ denotes the true (observed) number of new distinct users observed between day d_0 and day $d_0 + d$, given $Z1 : D_0$. Here, $1 \leq d_0 < D_0$, and $d_0 + d \leq D_0$. In our experiments, we find that the choice of $d_0 = 1$ works well, although in different applications, different choices might work better in practice (e.g., Masoero et al. (2022, Section 4) recommends $d_0 = \lfloor 2/3 \times D_0 \rfloor$).

The curve fitting approach offers two advantages compared to the maximum marginal likelihood one. First, it is much faster to evaluate numerically $\hat{U}_{d_0}^{(d)}$ compared to the log-likelihood, especially when the number of active users in the first D_0 days is large. Second, $\hat{U}_{d_0}^{(d)}$ does not depend on the whole sample, but only the simple sufficient statistics, (D_0, N_{D_0}) . Hence, curve fitting is feasible even when only first trigger counts, and not re-trigger counts, are available. This scenario might occur on proprietary or large datasets, where, e.g., for privacy reasons or reasons of scale, only aggregate summary statistics can be stored (e.g., the ASOS dataset later analyzed (Liu et al., 2021)). However, in our experience, maximum likelihood typically performs better in terms of predictive accuracy.

4.3 Empirics for parameter estimation

We provide here numerical evidence for both the maximum marginal likelihood and curve fitting approaches to parameter estimation. We consider specifically the NB-SSP model, as the Be-SSP one can be recovered by setting $r = 1$.

We generate $D = 365$ observations from the true model with fixed parameters $(\alpha, \beta, c, r) = (0.5, 2, 30, 5)$. fig. 9 in Appendix Section S5 shows the profile of the negative (log) likelihood function around the true value of the parameters. Specifically, in each subplot, we evaluate the negative log-likelihood in the right and left neighborhoods of the true value, shifting one coordinate at a time. We see that the negative log-likelihood is at least locally convex for all parameters. We adopt a derivative-free optimization routine, which empirically robustly finds good values of the hyperparameters for the prediction task at hand.

Next, we compare the performance of maximum marginal likelihood and curve-fitting on the unseen user prediction task. In particular, we measure the following accuracy metric, already defined in [Camerlenghi et al. \(2022\)](#):

$$v_{D_0}^{(D_1)} := 1 - \min \left\{ \frac{|U_{D_0}^{(D_1)} - \hat{U}_{D_0}^{(D_1)}|}{U_{D_0}^{(D_1)}}, 1 \right\}, \quad (14)$$

i.e., $v_{D_0}^{(D_1)}$ is one minus the relative prediction error. When the prediction is perfect, this metric equals 1 and degrades to 0 as its quality worsens.

To assess the performance of these two alternative empirical Bayes strategies, we consider synthetic data drawn from the NB-SSP model. For a fixed total duration $D = 500$, we draw samples $Z_{1:D} \sim \text{NB-SSP}$. For each $D_0 \in \{5, 10, 20, 50\}$, we retain $Z_{1:D_0}$ as a training set, and estimate the parameters α, β, c, r using either eq. (12) or eq. (13) and compute the corresponding accuracy $v_{D_0}^{(D-D_0)}$. We repeat this procedure $M = 100$ times (by re-drawing each time $Z_{1:D}$ from the prior), and report the median accuracy and a centered confidence interval with level 80% as D_0 increases, for three different choices of the hyperparameters (α, β, c, r) in fig. 3. While the confidence intervals greatly overlap, we can conclude that maximum marginal likelihood yields better predictive accuracy on average. Therefore, whenever possible, we advocate this approach. When re-trigger information is unavailable (e.g., for the ASOS data of [Liu et al. \(2021\)](#)), we adopt the regression approach.

Figure 3 reveals that when the data is generated from the true model even extremely small sample sizes allow us to form accurate predictions of future user activity. This is important, as experimenters typically want to form predictions in the early phases of the experiment.

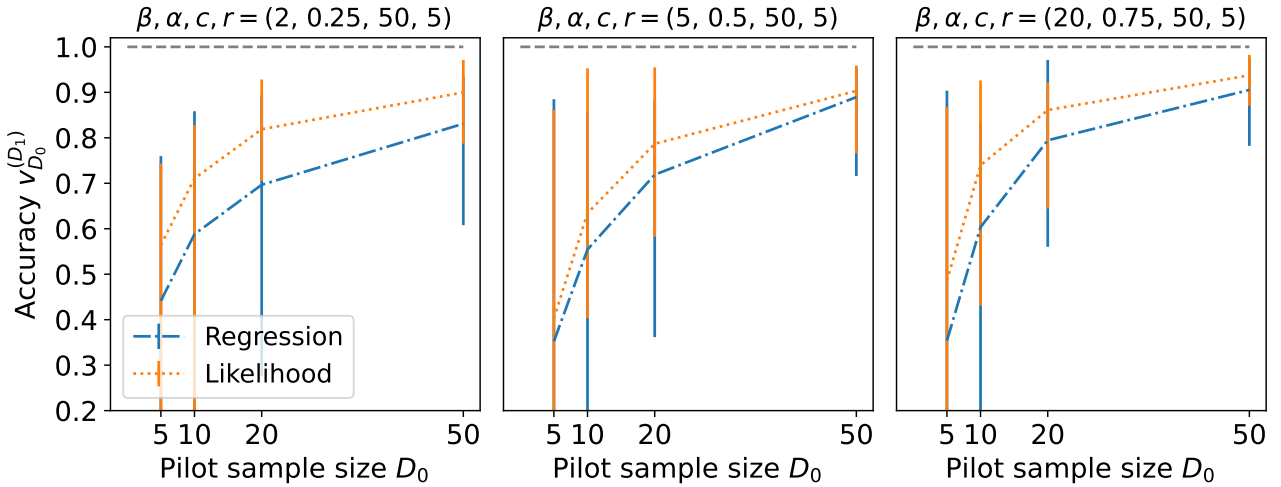


Figure 3: Prediction accuracy $v_{D_0}^{(D_1)}$ of the Bayesian nonparametric predictor on data from the model.

5 Simulation studies

We now evaluate the performance of our Bayesian nonparametric estimators via simulations on synthetic data, shedding light on several aspects of our models.

5.1 Prediction accuracy when the data is drawn from the true model

5.1.1 Binary activity data

We start with the simpler setting where activity data is binary — $A_{d,n} \in \{0, 1\}$. We consider two data generating processes: in the first (DG1) we simulate data from the Be-SSP model using the generative scheme detailed in Section S3. In the second (DG2), we first simulate data as in DG1, and retain only the first trigger event F_n for each user n . Then, for each user we simulate $\varepsilon_n \stackrel{\text{iid}}{\sim} \mathcal{U}([0, 0.5])$ and $A_{d,n} \sim \varepsilon_n \text{Be}((1 - \alpha)/(1 - \alpha + F_n))$ for $d > F_n$. That is, in DG2, after the first trigger, users tend to be less active.

For both data generating processes, we fix $D_0 = 14$, $c = 2500$, $\beta = 0.5$, and simulate 50 independent dataset that differ only in the value of $\alpha \sim \text{Beta}(4, 10)$. Note that these parameters values are used only to generate the synthetic datasets, while predictions are based on estimated parameters obtained by maximizing the marginal log-likelihood via eq. (12). Because the activity data is binary, we compare only the Be-SSP and TG-SSP models on the unseen user prediction task at $D_1 = 14$ follow-up days. Since both models lead to the same expression for $\hat{U}_{D_0}^{(D_1)}$ as in eq. (10), we are effectively comparing how well the numerical algorithms can recover the true data generating parameters when maximizing the marginal likelihoods under the two models.

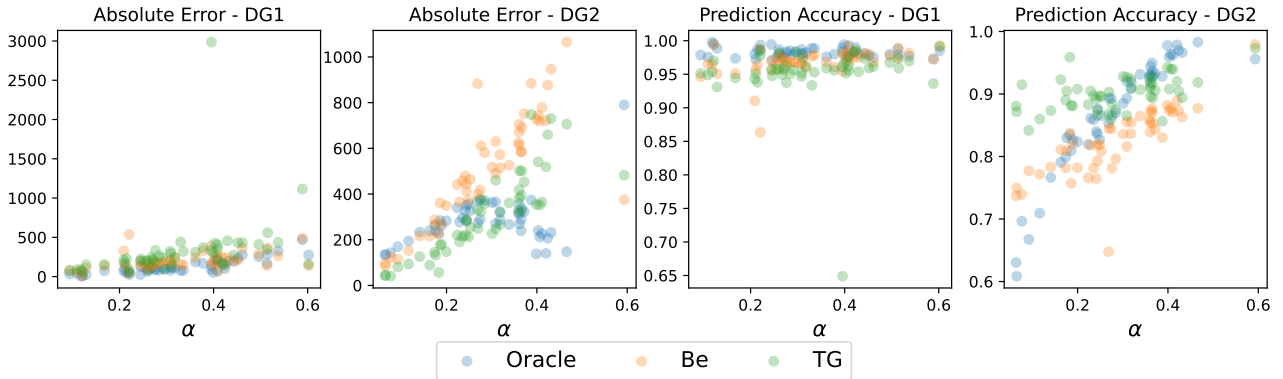


Figure 4: Absolute prediction error ($|U_{D_0}^{(D_1)} - \hat{U}_{D_0}^{(D_1)}|$) and accuracy ($v_{D_0}^{(D_1)}$) for the simulated scenarios described in Section 5.1.1.

We further compare our models to a Bayesian oracle who knows the data generating parameters and uses the expected value of $U_{D_0}^{(D_1)}$ for her predictions.

Figure 4 summarizes our findings. In DG1, the oracle estimator achieves the smallest errors. BM is competitive with the oracle while GM usually yields slightly larger errors. Looking at the relative errors, we can see that these are usually less than 10% and the three prediction yield comparable errors. In contrast, under DG2, GM performs significantly better (improvements are usually greater than 10% for the relative error) than BM across all values of α in the data generating process. Surprisingly, GM outperforms the oracle for smaller values of α as well. In summary, when the data follow the assumption of Be-SSP models (namely, each user is active on each given day with constant user-specific probability), the Bernoulli model is the best model but TG-SSP provides competitive estimates. Instead, when the data do not follow such assumptions, as in DG2, Be-SSP produces much poorer estimates than TG-SSP .

5.1.2 Count-valued activity data

We then move to the setting where activity data is count-valued, $A_{d,n} \in \mathbb{N}$. We draw synthetic the NB-SSP model introduced in definition 3.3. We sample $D = 200$ days worth of data $Z_{1:D}$ with parameters $(\beta, \alpha, c, r) = (0.1, 0.5, 50, 5)$. We retain the first $D_0 = 20$ days to fit the hyperparameters and form predictions for $U_{D_0}^{(d)}$ and $U_{D_0}^{(d,j)}$ by using the posterior mean induced by the fitted parameters, using the characterization provided in eq. (10). For all the statistics considered, we are able to form predictions to a high degree of accuracy.

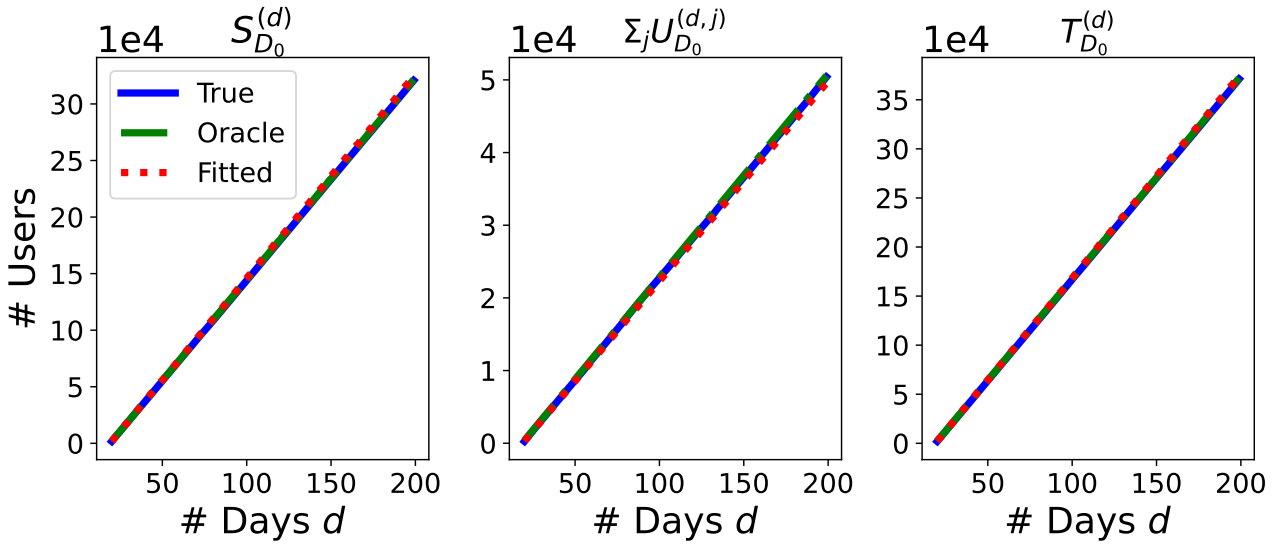


Figure 5: Prediction of future user activity (left, $S_{D_0}^{(d)}$, center, $\sum_j U_{D_0}^{(d,j)}$, right $T_{D_0}^{(d)}$). We plot the value of the statistic (vertical axis) as the number of days d increases (horizontal axis). We compare the true value in future samples (solid blue line) to the predicted posterior mean using the fitted (red) and the true (green) hyperparameters.

5.2 Prediction accuracy when the data is drawn from a Zipfian model

Next, we consider synthetic data from a Zipf-Poisson distribution. We evaluate the performance of our predictors against that of a collection of competing methods: the Jackknife estimator of order k (Jk) (Gravel, 2014), the linear programming approach of Zou et al. (2016), the Good-Toulmin estimator (Good, 1953), the Bayesian models of Ionita-Laza et al. (2009) (BB) and Richardson et al. (2022) (HBG), and the three-parameter Indian buffet process (IBP Teh and Gorur, 2009). In particular, for a given cardinality $N_\infty = 1,000,000$ of possible users we draw trigger data as follows. We endow each user n with a triggering rate $\theta_n = n^{-\tau}$, with $\tau = 0.6, 0.7, 0.8, 0.9$. Then, for every experimental day d , we determine whether each user n re-triggers by flipping a Bernoulli coin, $X_{d,n} \sim \text{Bernoulli}(\theta_n)$. Conditionally on $X_{d,n} = 1$, we sample $Z_{d,n} \sim \text{tPoisson}(1 + m_{d-1,n}/d; 0)$, where $m_{d-1,n}$ is the total re-trigger rate of unit n up to day $d-1$ and $\text{tPoisson}(a; b)$ is the law of a Poisson random variable with parameter a and supported on $\{b+1, b+2, \dots\}$. For each value τ , we generate $M = 100$ datasets. We retain only $D_0 = 5$ days for training, and compute the predictive accuracy $v_{D_0}^{(D_1)}$ for $D_1 = 50$ days ahead. Our results in Figure 6 show that across values of τ our method (Be-SSP) is competitive with the best alternatives in the literature, achieving a predictive performance comparable to the scaled-stable-beta-Bernoulli process (SSP) and the Indian buffet process (IBP). Each boxplot

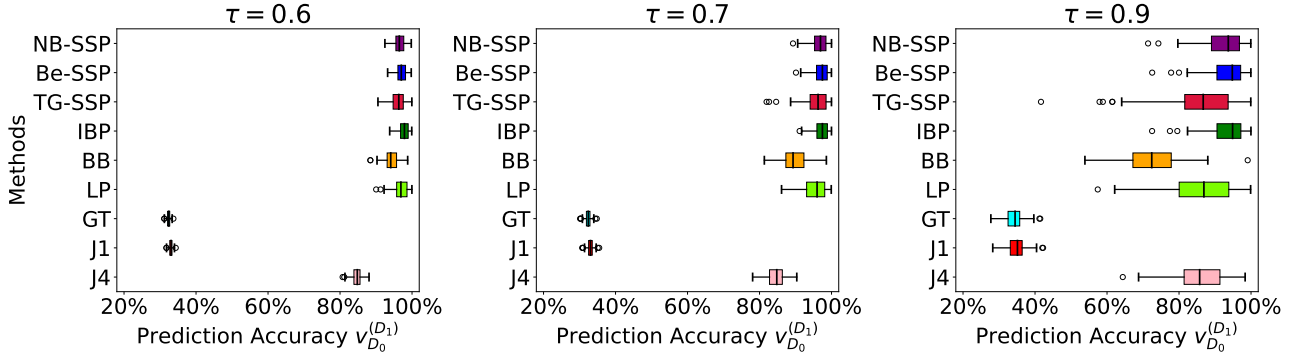


Figure 6: Prediction accuracy $v_{D_0}^{(D_1)}$ of predictors $\hat{U}_{D_0}^{(D_1)}$ on synthetic data from the Zipfian model for different choices of the parameter τ . Here, $D_0 = 10$ and $D_1 = 50$.

reports the median of the accuracy, together with a box of width given by the interquartile range.

Additionally, we show in Figure 10 in Appendix S5 that the total sum predictor $\hat{T}_{D_0}^{(D_1)}$ achieves great accuracy in predicting the total sum via a survival plot. While beyond the scope of the present paper, total re-trigger rates can be leveraged in forming better estimates of long-term treatment effects and to better predict the duration needed for an experiment to deliver significant results (Richardson et al., 2022; Wan et al., 2023). To this end, we define a notion of accuracy for the prediction of the total retrigger rates $\hat{T}_{D_0}^{(D_1)}$:

$$\tilde{v}_{D_0}^{(D_1)} := 1 - \min \left\{ \frac{|t_{D_0}^{(D_1)} - \hat{T}_{D_0}^{(D_1)}|}{t_{D_0}^{(D_1)}}, 1 \right\} \in [0, 1].$$

$t_{D_0}^{(D_1)}$ is the observed total retrigger rate between D_0 and $D_0 + D_1$

5.3 Estimating the days to a given participation threshold

We consider here the estimation of D_M and compare the two approaches outlined in Section 3.4. We consider only the TG-SSP model. Analogous results hold for the other models presented in the paper.

We simulate data $X_{d,n}$ as in Section 5.2, for $\tau = 0.8, 1.0, 1.2, 1.4$. We generate data for $D_0 = 14$ days, thus observing N_{D_0} users, and we want to estimate the number of days needed to get ηN_{D_0} users for $\eta = 1.5, 2.0, 5.0$.

We compare the intervals for D_M based on the inversion technique depicted in Figure 1 with the posterior mean and 95% credible intervals obtained from the posterior of D_M , which is approximated using 1,000 draws from Algorithms 1. The intervals obtained via the inversion

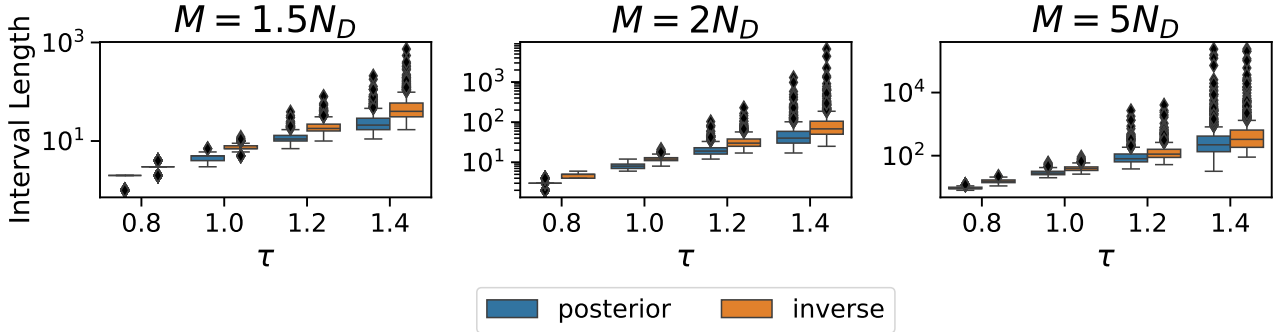


Figure 7: Length of the prediction intervals for D_M for 500 simulated datasets according to the simulation in Section 5.3. Different plots correspond to different values of M . In each plot, the parameter τ of the data generating process varies across the horizontal axis.

techniques are wider than those based on the posterior of D_M , see Figure 7. Moreover, the length of the intervals increases with parameter τ of the data generating process. This is intuitive: for smaller values of τ we expect to see more users in the first days while if τ is larger it might require hundreds or thousands of days to reach the desired number of users. As far as the calibration of the intervals is concerned, when $M = 5N_{D_0}$ or $\tau = 1.4$ both types of intervals are misscalibrated, their coverage varying from 60% to 90% depending on the setting. Instead, for $M = 1.5N_{D_0}, 2N_{D_0}$ and $\tau \leq 1.0$ the posterior of D_M produces (almost) perfectly calibrated intervals, while the inversion intervals have a coverage above the nominal level, as expected given that the inversion intervals are larger. Finally, when $\tau = 1.2$, the coverage of the inversion intervals is slightly below the nominal level (around 93%) while the posterior inference intervals have a coverage of 90% (when $M = 1.5N_{D_0}$) and 85% (when $M = 2N_{D_0}$).

Concerning the computational costs of producing the intervals, we note the following. To generate a draw from the posterior of D_M , we use Algorithm 1. While a big-O analysis of such an algorithm eludes us, we can comment that the number of support points of \tilde{F} , i.e., ξ using notation of Theorem 3.8 seems to grow linearly with the parameter D^{up} . Then one needs to sample F'_ℓ , $\ell = 1, \dots, \xi$, from a discrete distribution over $\{D_0 + 1, \dots, D_0 + D^{up}\}$, which requires computing D^{up} probabilities. In summary, Algorithm 1 can be seen to scale quadratically in D^{up} . Instead, the inversion approach requires computing the global credible band, that needs to sample repeatedly from the law of N_ℓ^* , $\ell = 1, \dots, D^{up}$ in Proposition 3.6, compute the density of the samples and evaluate the trajectories for $N_{D_0+\ell}$, all of which scales linearly in D^{up} . Most importantly, the computational cost of estimating the inverse interval for D_M is not affected by the value of α . On the other hand, for large values of α , the value of ξ in Algorithm 1 can

be seen to increase steeply. To test these insights, we performed a small simulation where we generated data from (DG2) for $D_0 = 7$ days, with fixed parameters $\beta = 0.5$, $c = 1000$ and $\alpha = 0.25, 0.5, 0.75$. We then tried to compute the inversion and posterior intervals of D_M with $M = 2N_{D_0}$. Computing the inversion intervals took around 0.1s across all simulations, while for the posterior intervals the cost ranged from 0.2s (when $\alpha = 0.25$) to almost 10s (when $\alpha = 0.75$).

6 Real data analyses

We last assess the empirical performance of our and competing methods on real data. We analyze three datasets. The first is a proprietary dataset consisting of trigger data from a large meta-analysis containing 1,774 experiments run in production by a large technology company of varying size (from small experiments with a few thousand users to large experiments with hundreds of million users per experiment). The second dataset is the ASOS dataset provided in [Liu et al. \(2021\)](#), from which we retain 76 treatment arms across experiments. The third dataset consists of a subset of 50 experiments from the first dataset for which users' re-trigger data have been collected.

In particular, the first dataset contains information about the number of users that triggered on any given day. Therefore, on this data, parameter estimation via maximum marginal is feasible only for the Be-SSP and TG-SSP models but not for the NB-SB-SP one. We also fit the parameters of BB and IBP via maximum marginal likelihood. The ASOS data, instead, only provides for each experiment the number of distinct users first triggering on a given date. Therefore, we only consider the Bayesian models, which can be trained with the available data via maximum marginal likelihood or curve fitting. For both datasets, we retain $D_0 = 7$ days worth of pilot data and predict the number of users at either $D_1 = 21$ days ahead (proprietary data) or at the last available time point (ASOS data). For the third dataset, we use the NB-SB-SP model to predict the total activity rate by considering $D_0 = 7$ days of pilot data.

The ASOS data ([Liu et al., 2021](#)) only provides for each experiment the number of distinct users first triggering on a given date, and not the number of users who retrigged a given number of times throughout the experiment, information needed to fit other competing methods (see Section S4 for additional details). We therefore only consider the Bayesian models which can be trained with the available data. Again, the NB-SB-SP is competitive with the best available alternative.

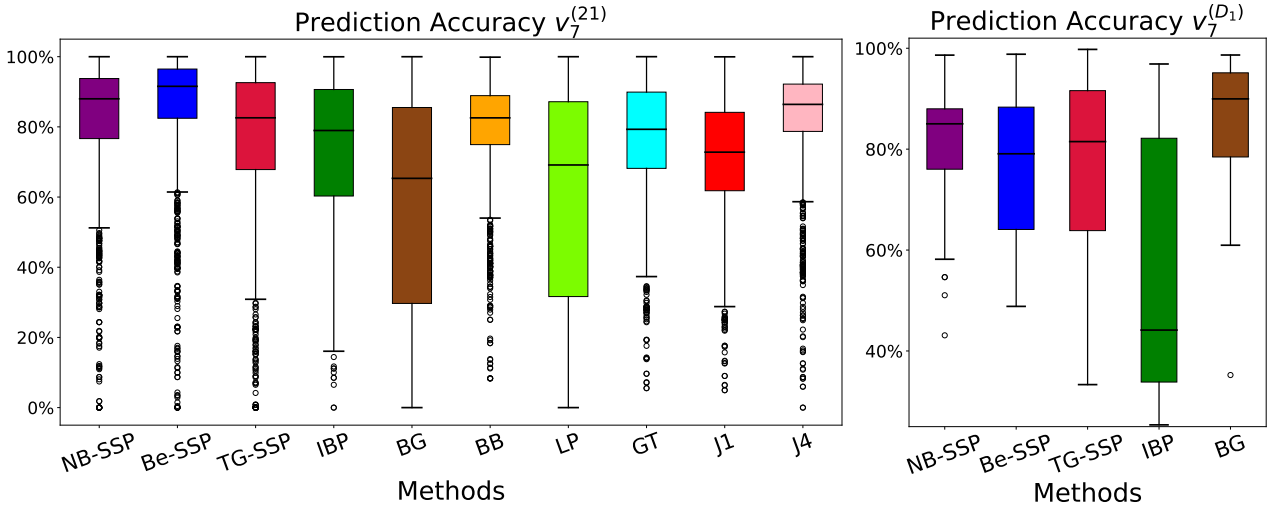


Figure 8: Prediction accuracy on proprietary (left) and ASOS (right) data.

Last, we assess in Figure 11 in Appendix Section S5 the performance of our method on a smaller subset of 50 experiments at predicting the total future activity rate. We retain $D_0 = 7$ days for training, and extrapolate at different horizons $D_1 = 14, 21, 28, 35$. For this task, no alternative method is available.

7 Discussion

This paper presents a novel Bayesian nonparametric framework for predicting user engagement in online A/B tests using stable beta-scaled process priors. While the theoretical foundation draws from rather complex random measure theory, the resulting methodology yields tractable, closed-form estimators that can be readily implemented by practitioners. This accessibility is particularly valuable in industrial settings, where rapid decision-making about experiment duration and resource allocation is critical.

A key strength of our approach lies in its computational efficiency. Indeed, the posterior distributions and predictive quantities have explicit expressions that avoid the need for costly MCMC sampling. The hyperparameter optimization, performed through maximum marginal likelihood or curve fitting, is straightforward and robust. This combination of theoretical rigor and computational tractability makes our method particularly appealing for large-scale applications where thousands of experiments may need to be analyzed simultaneously.

Our empirical results demonstrate that the proposed models - Be-SSP, TG-SSP, and NB-SSP - can effectively capture different aspects of user behavior. The Be-SSP and TG-SSP

models are well-suited for coarse activity data, while the NB-SSP model provides additional flexibility for analyzing granular engagement patterns. The superior performance of our approach compared to existing methods, particularly in scenarios with limited pilot data, suggests that the stable beta-scaled process prior effectively captures the power-law behavior often observed in user engagement data.

The methodology introduced here extends beyond the specific context of online A/B testing. The flexible framework can be adapted to other domains where predicting user engagement is crucial, such as customer retention analysis and churn prediction. Moreover, our approach to handling both coarse and granular activity data provides a template for developing similar methodologies in other applications where data may be available at different levels of resolution.

This work suggests several directions for future research. First, extending the models to incorporate user covariates could provide more nuanced predictions based on user characteristics or experimental conditions. Second, our models treat each arm of the A/B test independently. However, the first triggering time of users is independent of the treatment, which affects only the re-trigger rates. This kind of dependence is not captured by standard nonparametric priors, such as the ones based on hierarchical or nested processes, and will be the object of future investigation.

In conclusion, this work demonstrates that sophisticated Bayesian nonparametric methods can be made practically accessible without sacrificing theoretical rigor. The methods presented here provide experimenters with reliable tools for predicting user engagement and making informed decisions about experiment duration, while opening new avenues for theoretical research in Bayesian nonparametrics and their applications to large-scale experimentation.

References

Beraha, M. and S. Favaro (2023). Transform-scaled process priors for trait allocations in Bayesian nonparametrics. *arXiv preprint arXiv:2303.17844*.

Broderick, T., M. I. Jordan, and J. Pitman (2012). Beta Processes, Stick-Breaking and Power Laws. *Bayesian Analysis* 7(2), 439 – 476.

Burnham, K. P. and W. S. Overton (1979). Robust estimation of population size when capture probabilities vary among animals. *Ecology* 60(5), 927–936.

Camerlenghi, F., S. Favaro, L. Masoero, and T. Broderick (2022). Scaled process priors for

Bayesian nonparametric estimation of the unseen genetic variation. *Journal of the American Statistical Association*, 1–12.

Campbell, T., D. Cai, and T. Broderick (2018). Exchangeable trait allocations. *Electronic Journal of Statistics* 12(2), 2290 – 2322.

Carlin, B. P. and T. A. Louis (2000). Empirical Bayes: Past, present and future. *Journal of the American Statistical Association* 95(452), 1286–1289.

Chakraborty, S., A. Arora, C. B. Begg, and R. Shen (2019). Using somatic variant richness to mine signals from rare variants in the cancer genome. *Nature communications* 10(1), 5506.

Deng, A. (2015). Objective Bayesian two sample hypothesis testing for online controlled experiments. In *Proceedings of the 24th International Conference on World Wide Web*, pp. 923–928.

Efron, B. and R. Thisted (1976). Estimating the number of unseen species: How many words did Shakespeare know? *Biometrika* 63(3), 435–447.

Ferguson, T. S. and M. J. Klass (1972). A Representation of Independent Increment Processes without Gaussian Components. *The Annals of Mathematical Statistics* 43(5), 1634 – 1643.

Good, I. J. (1953). The population frequencies of species and the estimation of population parameters. *Biometrika* 40(3-4), 237–264.

Good, I. J. and G. H. Toulmin (1956). The number of new species, and the increase in population coverage, when a sample is increased. *Biometrika* 43(1-2), 45–63.

Gravel, S. (2014). Predicting discovery rates of genomic features. *Genetics* 197(2), 601–610.

Griffiths, T. L. and Z. Ghahramani (2011). The Indian buffet process: An introduction and review. *Journal of Machine Learning Research* 12(32), 1185–1224.

Gupta, S., R. Kohavi, D. Tang, Y. Xu, R. Andersen, E. Bakshy, N. Cardin, S. Chandran, N. Chen, D. Coey, et al. (2019). Top challenges from the first practical online controlled experiments summit. *ACM SIGKDD Explorations Newsletter* 21(1), 20–35.

Ionita-Laza, I., C. Lange, and N. M. Laird (2009). Estimating the number of unseen variants in the human genome. *Proceedings of the National Academy of Sciences* 106(13), 5008–5013.

James, L. F. (2017). Bayesian Poisson calculus for latent feature modeling via generalized Indian Buffet Process priors. *The Annals of Statistics* 45(5), 2016 – 2045.

James, L. F., P. Orbanz, and Y. W. Teh (2015). Scaled subordinators and generalizations of the Indian buffet process. *arXiv: Probability*.

Kingman, J. F. C. (1967). Completely random measures. *Pacific Journal of Mathematics* 21(1), 59 – 78.

Kohavi, R., A. Deng, B. Frasca, T. Walker, Y. Xu, and N. Pohlmann (2013). Online controlled experiments at large scale. In *Proceedings of the 19th ACM SIGKDD international conference on Knowledge discovery and data mining*, pp. 1168–1176.

Liu, C. H. B., Â. Cardoso, P. Couturier, and E. J. McCoy (2021). Datasets for online controlled experiments. In *Thirty-fifth Conference on Neural Information Processing Systems Datasets and Benchmarks Track (Round 2)*.

Masoero, L., F. Camerlenghi, S. Favaro, and T. Broderick (2018). Posterior representations of hierarchical completely random measures in trait allocation models. In *NeurIPS Workshop on All of Bayesian Nonparametrics*.

Masoero, L., F. Camerlenghi, S. Favaro, and T. Broderick (2022). More for less: predicting and maximizing genomic variant discovery via Bayesian nonparametrics. *Biometrika* 109(1), 17–32.

Quenouille, M. H. (1956). Notes on bias in estimation. *Biometrika* 43(3/4), 353–360.

Richardson, T. S., Y. Liu, J. McQueen, and D. Hains (2022, 28–30 Mar). A Bayesian model for online activity sample sizes. In G. Camps-Valls, F. J. R. Ruiz, and I. Valera (Eds.), *Proceedings of The 25th International Conference on Artificial Intelligence and Statistics*, Volume 151 of *Proceedings of Machine Learning Research*, pp. 1775–1785. PMLR.

Storn, R. and K. Price (1997). Differential evolution—a simple and efficient heuristic for global optimization over continuous spaces. *Journal of global optimization* 11, 341–359.

Teh, Y. and D. Gorur (2009). Indian buffet processes with power-law behavior. In Y. Bengio, D. Schuurmans, J. Lafferty, C. Williams, and A. Culotta (Eds.), *Advances in Neural Information Processing Systems*, Volume 22. Curran Associates, Inc.

Tukey, J. (1958). Bias and confidence in not quite large samples. *Ann. Math. Statist.* 29, 614.

Wan, R., Y. Liu, J. McQueen, D. Hains, and R. Song (2023). Experimentation platforms meet reinforcement learning: Bayesian sequential decision-making for continuous monitoring. In *Proceedings of the 29th ACM SIGKDD Conference on Knowledge Discovery and Data Mining*, pp. 5016–5027.

Zou, J., G. Valiant, P. Valiant, K. Karczewski, S. O. Chan, K. Samocha, M. Lek, S. Sunyaev, M. Daly, and D. G. MacArthur (2016). Quantifying unobserved protein-coding variants in human populations provides a roadmap for large-scale sequencing projects. *Nature communications* 7(1), 13293.

Supplementary material for:
 “Online activity prediction via generalized Indian buffet
 process models”

Organization of the supplementary material

The supplementary material is organized as follows. Section [S1](#) provides the necessary background on Bayesian nonparametrics and states the main results used in our proofs. Section [S2](#) collects the proofs of our theoretical results and Section [S5](#) reports additional plots not included in the main manuscript.

S1 Background Material on Bayesian nonparametrics and Random Measures

A completely random measure (CRM) on Ω (with associated σ -algebra) is a random element μ taking values in the space of (finite) measures over Ω (with associated Borel σ -algebra) such that for any n and any collection of disjoint subsets A_1, \dots, A_n of Ω , the random variables $\mu(A_1), \dots, \mu(A_n)$ are independent. It is well-known ([Kingman, 1967](#)) that a CRM can be decomposed as a sum of a deterministic measure, an atomic measure with fixed atoms and random jumps, and an atomic measure where both atoms and jumps are random and form the points of a Poisson point process. As customary in BNP, here we discard the deterministic parts of CRMs and consider measures of the form $\mu(\cdot) = \int_{\mathbb{R}_+} sN(ds, \cdot) = \sum_{k \geq 1} \tau_k \delta_{\omega_k}(\cdot)$, where $N = \sum_{k \geq 1} \delta_{(\tau_k, \omega_k)}$ is a Poisson random measure on $\mathbb{R}_+ \times \Omega$ with Lévy intensity measure $\nu(ds, dx)$. The Lévy intensity characterizes the distribution of μ via the Lévy-Khintchine representation of its Laplace functional. That is, for measurable $f : \Omega \rightarrow \mathbb{R}_+$

$$\mathbb{E} \left[e^{- \int_{\Omega} f(x) \mu(dx)} \right] = \exp \left\{ - \int_{\mathbb{R}_+ \times \Omega} (1 - e^{-sf(x)}) \nu(ds dx) \right\}.$$

Our focus is on homogeneous Lévy intensity measures, namely measures of the form $\nu(ds, dx) = \theta \rho(s) ds P_0(dx)$ where $\theta > 0$ is a parameter, P_0 is a nonatomic probability measure on Ω and $\rho(s) ds$ is a measure on \mathbb{R}_+ such that $\int_{\mathbb{R}_+} \rho(ds) = +\infty$ and $\psi(u) := \int_{\mathbb{R}_+} (1 - e^{-us}) \rho(s) ds < +\infty$ for all $u > 0$. These conditions ensure that $0 < \mu(\mathbb{W}) < +\infty$ almost surely. We write

$\mu \sim \text{CRM}(\theta, \rho, P_0)$. Under a trait allocation model, the law of μ provides a natural prior distribution for the parameter of the trait process.

We recall below the main results due to [James \(2017\)](#) for the Bayesian analysis of trait allocations under a CRM prior. Consider the trait allocations $X_j = \sum_{k \geq 1} X_{j,k} \delta_{\omega_k}$, $j = 1, \dots, n$. Given $\mu = \sum_{k \geq 1} \tau_k \delta_{\omega_k}$ we assume that

- for each k , $X_{j,k} | \mu \stackrel{\text{iid}}{\sim} G(\cdot | \tau_k)$ where $G(\cdot | s)$ is a distribution over the nonnegative integers such that $\pi_G(s) := G(0 | s) > 0$
- the variables $X_{j,k}$ are independent across k , given μ
- μ is a completely random measure with Lévy intensity $\nu(ds dx) = \theta \rho(s) ds P_0(dx)$.

We use the short-hand notation

$$X_j = \sum_{k \geq 1} X_{j,k} \delta_{\omega_k} | \mu \stackrel{\text{iid}}{\sim} \text{TrP}(G; \mu), \quad \mu \sim \text{CRM}(\theta, \rho, P_0) \quad (\text{S1})$$

and further define

$$\varphi_k = \theta \int_{\mathbb{R}_+} \pi_G(s) (1 - \pi_G(s))^{k-1} \rho(s) ds.$$

Proposition S1.1 (Marginal law, Proposition 3.1 in [James \(2017\)](#)). *Let X_1, \dots, X_n be distributed as (S1), such that the sample displays traits $\omega_1^*, \dots, \omega_k^*$ and let $\mathcal{B}_j = \{i : X_i(\omega_j^*) > 0\}$, $|\mathcal{B}_j| = m_j$. Then, the marginal law of (X_1, \dots, X_n) is*

$$\theta^k e^{-\sum_{i=1}^n \varphi_i} \prod_{j=1}^k \int_{\mathbb{R}_+} (1 - \pi_G(s))^{n-m_j} \prod_{i \in \mathcal{B}_j} G(a_{i,j} | s) \rho(s) ds.$$

Theorem S1.2 (Posterior law, Theorem 3.1 in [James \(2017\)](#)). *Let X_1, \dots, X_n be distributed as (S1), such that the sample displays traits $\omega_1^*, \dots, \omega_k^*$ and let $\mathcal{B}_j = \{i : X_i(\omega_j^*) > 0\}$, $|\mathcal{B}_j| = m_j$. Then, the posterior distribution of μ is equivalent to the distribution of*

$$\sum_{j=1}^k J_j^* \delta_{\omega_j^*} + \mu'$$

where

1. J_j^* are independent positive random variables, also independent of μ' with density

$$f_j(s) \propto (1 - \pi_G(s))^{n-m_j} \prod_{i \in \mathcal{B}_j} G(a_{i,j} | s) \rho(s)$$

2. μ' is a completely random measure with Lévy intensity

$$(1 - \pi_G(s)^{n-1} \rho(s) ds) P_0(dw)$$

Proposition S1.3 (Compound Poisson representation, Proposition 3.3 in [James \(2017\)](#)). *Let X be as in (S1). Then the law of X is equivalent to the distribution of*

$$\sum_{j=1}^K \tilde{A}_j \delta_{\tilde{\omega}_k}$$

where $K \sim Poi(\varphi_1)$, $\tilde{\omega}_k \stackrel{iid}{\sim} P_0$ and the \tilde{A}_k 's are independent random variables with values in $\{1, 2, \dots\}$ given by

$$\Pr(A_k = a) \propto \int G(a | s) \rho(s) ds$$

S2 Proofs

We will need the following technical lemma, which follows trivially from Lemma 1 in [Camerlenghi et al. \(2022\)](#)

Lemma S2.1. *Let $\tilde{\mu} \sim SB\text{-}SP(\alpha, c, \beta)$. Then, the law of $\tilde{\mu} | \Delta_{1,h}$ equals the one of a CRM with Lévy intensity*

$$\Delta_{1,h}^{-\alpha} \alpha s^{-1-\alpha} I_{[0,1]}(s) ds P_0(dx)$$

Proof of Theorem 3.4. The proof follows by combining Theorem S1.2 and Lemma S2.1.

In particular, by standard disintegration arguments

$$\mathcal{L}(\tilde{\mu} | Z_{1:D}) = \mathbb{E}[\mathcal{L}(\tilde{\mu} | Z_{1:D}, \Delta_{1,h}) | Z_{1:D}]$$

and we can further introduce a positive-valued random variable $\tilde{\Delta}_{1,h}$ with law $\mathcal{L}(\Delta_{1,h} | Z_{1:D})$ to obtain

$$\mathcal{L}(\tilde{\mu} | Z_{1:D}) = \int_{\mathbb{R}_+} \mathcal{L}(\tilde{\mu} | Z_{1:D}, \tilde{\Delta}_{1,h}) \mathcal{L}(d\tilde{\Delta}_{1,h}).$$

Then, the term $\mathcal{L}(\tilde{\mu} | Z_{1:D}, \tilde{\Delta}_{1,h})$ can be obtained by observing that $\tilde{\mu} | \Delta_{1,h}$ is a CRM as in Lemma S2.1 so that $\mathcal{L}(\tilde{\mu} | Z_{1:D}, \Delta_{1,h})$ is the posterior distribution described in Theorem S1.2. That is

$$\tilde{\mu} | \tilde{\Delta}_{1,h} = \sum_{n=1}^{N_D} \theta_n^* \delta_{\omega_n^*} + \mu'$$

where $\theta_n^* | \tilde{\Delta}_{1,h}$ are independent with density

$$f_{\theta_n^*}(\theta | \tilde{\Delta}_{1,h}) \propto (1 - \pi_{\mathcal{G}}(\theta))^{D-m_n} \theta^{-1-\alpha} \prod_{d \in \mathcal{B}_n} \mathcal{G}(A_{d,n}; \theta)$$

which does not depend on $\tilde{\Delta}_{1,h}$. Moreover, $\mu' | \tilde{\Delta}_{1,h}$ is as in the statement of the theorem.

It remains to obtain the law of $\tilde{\Delta}_{1,h} \stackrel{d}{=} \Delta_{1,h} | Z_{1:D}$. An application of Bayes' rule yields that the density of $\tilde{\Delta}_{1,h}$ is

$$f_{\tilde{\Delta}_{1,h}}(\zeta) \propto \Pr(Z_1, \dots, Z_D | \Delta_{1,h} = \zeta) h_{\alpha, c, \beta}(\zeta)$$

where $\Pr(Z_1, \dots, Z_D | \Delta_{1,h})$ is the joint distribution of $Z_{1:D}$ given $\Delta_{1,h}$, whose expression can be obtained by combining Proposition S1.1 and Lemma S2.1. Simple algebra yields the result. \square

Proof of Corollary 3.5. The proof follows by the definition of Beta function and simple algebra. \square

Proof of Proposition 3.6. The main idea is to first condition of $\Delta_{1,h}$ and exploit the general results in James (2017). We present the proof for the TG-SSP model but computations are unchanged for the other models.

Let $Y' = \sum_{i \geq 1} Y'_i \delta_{\omega'_i}$ be the first triggering times of users that are active for the first time in the days $\{D_0 + 1, \dots, D_0 + D_1\}$. Then, by virtue of Corollary 3.5, $Y' | Y$ is distributed as

$$\begin{aligned} Y' | \tilde{\mu}' &\sim \text{TrP}(\text{TGeom}_{D_0+1}^{D_0+D_1}) \\ \tilde{\mu} | \Delta_{1,h} &\sim CRM(\Delta_{1,h}^{-\alpha} \alpha (1-s)^d s^{-1-\alpha} ds P_0(dx)) \\ \Delta_{1,c,\beta}^{-\alpha} &\sim \text{Gamma}(N_d + c + 1, \beta + \gamma_d). \end{aligned} \tag{S2}$$

Hence, given $\Delta_{1,h}$, Y' can be represented via Proposition S1.3 as

$$Y' | \Delta_{1,h}, Y = \sum_{i=1}^{K_{D_1}} \tilde{Y}_i \delta_{\tilde{\omega}_i}$$

where $K_{D_1} \sim \text{Poi}(\alpha \Delta_h^{-\alpha} \sum_{j=1}^{D_1} B(1-\alpha, D_0+j)) \equiv \text{Poi}(\alpha \Delta_h^{-\alpha} \psi_1(D_0, D_1))$.

Consider now Y'' be the triggering times of users first active on days $\{D_0 + D_1 + 1, \dots, D_0 + D_1 + D_2\}$. Arguing as above it is clear that, given $\Delta_{1,h}, Y$ and Y' ,

$$Y'' | \Delta_{1,h}, Y, Y' = \sum_{i=1}^{K_{D_2}} \tilde{Y}_i \delta_{\tilde{\omega}_i}$$

where now $K_{D_2} \sim \text{Poi}(\alpha \Delta_{1,h}^{-\alpha} \sum_{j=1}^{D_2} B(1-\alpha, D_0+D_1+j)) \equiv \text{Poi}(\alpha \Delta_{1,h}^{-\alpha} \psi_1(D_0+D_1, D_0+D_1+D_2))$. In particular, the law of K_{D_2} does not depend on Y' given $\Delta_{1,h}$. Taking $D_1 = D_2 = 1$ and reasoning by induction proves verifies the statement regarding N_ℓ^* .

To obtain the law of $U_{D_0}^{(D_1)}$, we exploit the closeness of the Poisson family under convolution and write $U_{D_0}^{(D_1)} = \sum_{\ell=1}^D N_\ell^*$, so that

$$U_{D_0}^{(D_1)} | \Delta_{1,h} \sim \text{Poi}(\alpha \Delta_{1,c,\beta}^{-\alpha} \psi_1(D_0, D_1)).$$

The results follows by integrating with respect to $\Delta_{1,h}^{-\alpha} \sim \text{Gamma}(N_D + c + 1, \beta + \psi_1(0, D_0))$. \square

Proof of Proposition 3.7. The only non-trivial statement concerns the distribution of $U_{D_0}^{(D_1,j)}$. Indeed, the representation follows by definition and the law of $S_{D_0}^{(D_1)}$ follows directly by Corollary 3.5. Similarly, the Bayesian estimator for $T_{D_0}^{(D_1)}$ is obtained by the linearity of expectations.

To prove that

$$U_{D_0}^{(D_1,j)} | Z_{1:D_0} \sim \text{NegBin}(N_{D_0} + c + 1, p_{D_0}^{(D_1,j)}),$$

we apply the argument in [Camerlenghi et al. \(2022, Theorem 2\)](#). Notice that the distribution of the new customers conditionally on the largest jump must be a Poisson distribution from the properties of CRMs. We can write from the predictive representation in (8)

$$U_{D_0}^{(D_1,j)} | Z_{1:D_0}, \Delta_{1,h} \stackrel{d}{=} \sum_{n \geq 1} I \left(\sum_{d=1}^{D_1} A'_{D_0+d,n} = j \right).$$

Here $A'_{D_0+d,n}$ is — conditionally on $\tilde{\mu}$ — a negative binomial random variable with parameters r, θ'_n , where θ'_n are the jumps of a Poisson point process with Lévy intensity

$$\tilde{\lambda}(s)ds = \alpha \Delta_{1,h_{\beta,c}}^{-\alpha} (1-s)^{rD_0} s^{-1-\alpha} \stackrel{\text{ind}}{\sim} (s \in (0,1))ds.$$

Now observing that the random variable

$$S_{D_0, D_1, n} := \sum_{d=1}^{D_1} A'_{D_0+d,n}$$

is a sum of i.i.d. negative binomial random variables with parameters r, θ'_n conditionally on $\tilde{\mu}$, it

holds that $S_{D_0, D_1, n} | \tilde{\mu} \sim \text{NegBin}(D_1 r, \theta'_n)$. It follows that

$$\begin{aligned}
\mathbb{E} \left[t^{U_{D_0}^{(D_1, j)}} | Z_{1:D_0}, \tilde{\mu} \right] &= \mathbb{E} \left[\mathbb{E} \left[\prod_{n \geq 1} \left\{ (t-1) \stackrel{\text{ind}}{\sim} \left(\sum_{d=1}^{D_1} A'_{D_0+d, n} = j \right) + 1 \right\} | \tilde{\mu} \right] \right] \\
&= \mathbb{E} \left[\prod_{n \geq 1} \left\{ (t-1) \Pr(S_{D_0, D_1, n} = j) + 1 \right\} \right] \\
&= \mathbb{E} \left[\prod_{n \geq 1} \left\{ (t-1) \binom{j+rD_1+1}{j} (\theta'_n)^j (1-\theta'_n)^{rD_1} + 1 \right\} \right] \\
&= \mathbb{E} \left[\exp \left\{ \sum_{n \geq 1} \log \left\{ (t-1) \binom{j+rD_1+1}{j} (\theta'_n)^j (1-\theta'_n)^{rD_1} + 1 \right\} \right\} \right] \\
&= \exp \left\{ -(1-t) \Delta_{1,h}^{-\alpha} \binom{j+rD_1+1}{j} \alpha \int (1-s)^{r(D_0+D_1)} s^{j-\alpha-1} ds \right\} \\
&= \exp \left\{ -(1-t) \Delta_{1,h}^{-\alpha} \binom{j+rD_1+1}{j} \alpha B[r(D_0+D_1)+1, j-\alpha] \right\} \\
&= \exp \left\{ -(1-t) \Delta_{1,h}^{-\alpha} \rho_{D_0}^{(D_1, j)} \right\},
\end{aligned}$$

with $\rho_{D_0}^{(D_1, j)} := \binom{j+rD_1+1}{j} \alpha B[r(D_0+D_1)+1, j-\alpha]$. One can then integrate with respect to the posterior distribution of $\Delta_{1,h}^{-\alpha}$ to obtain the final result:

$$\begin{aligned}
\mathbb{E} \left[t^{U_{D_0}^{(D_1, j)}} | Z_{1:D_0} \right] &= \frac{(\beta + \psi_0^{(D_0)})^{N+c+1}}{\Gamma(N+c+1)} \int_0^\infty \exp \left\{ -x(1-t) \rho_{D_0}^{(D_1, j)} \right\} x^{N+c} dx \\
&= \left(\frac{\beta + \psi_0^{(D_0)}}{\beta + \psi_0^{(D_0)} + \rho_{D_0}^{(D_1, j)} - t \rho_{D_0}^{(D_1, j)}} \right)^{N+c+1} \\
&= \left(\frac{1 - p_{D_0}^{(D_1, j)}}{1 - t p_{D_0}^{(D_1, j)}} \right)^{N+c+1}
\end{aligned}$$

for any $t < 1/|p_{D_0}^{(D_1, j)}|$, with

$$p_{D_0}^{(D_1, j)} := \frac{\rho_{D_0}^{(D_1, j)}}{\beta + \psi_0^{(D_0)} + \rho_{D_0}^{(D_1, j)}} \leq 1.$$

This is the probability generating function of a negative binomial distribution with success rate $p_{D_0}^{(D_1, j)}$ and $N+c+1$ failures:

$$\Pr(U_{D_0}^{(D_1)} = \ell | Z_{1:D_0}) = \binom{\ell + N + c}{\ell} (p_{D_0}^{(D_1, j)})^\ell (1 - p_{D_0}^{(D_1, j)})^{N+c+1} \quad \{\ell \in \mathbb{N}\}.$$

□

Proof of Theorem 3.8. The proof follows arguing as above, so we give here only a sketch. First, conditional to $\Delta_{1,h}$ we apply Proposition S1.3 which yields the representation as a counting

measure over a random number of support points. The law of \tilde{Y}'_ℓ and ω'_ℓ can be seen to be independent of $\Delta_{1,h}$ with the distributions reported in the statement. Finally, $\xi \mid \Delta_{1,h}$ follows a Poisson distribution as in Proposition S1.3, so that marginally it is negative-binomial distributed with parameters as in the statement. \square

Proof of Theorem 4.1. By the law of total expectation

$$\Pr(Z_1, \dots, Z_{D_0}) = \mathbb{E}[\Pr(Z_1, \dots, Z_{D_0} \mid \Delta_{1,h})]$$

where the argument inside the expectation is given by Proposition S1.1. In particular, it is straightforward to check that

$$\Pr(Z_1, \dots, Z_{D_0} \mid \Delta_{1,h}) = (\alpha \Delta_{1,h}^{-\alpha})^{N_{D_0}} e^{\psi_r(0, D_0) \Delta_{1,h}^{-\alpha}} \prod_{n=1}^{N_{D_0}} \Theta_n.$$

The result then follows by marginalizing with respect to $\Delta_{1,h}^{-\alpha} \sim \text{Gamma}(c, \beta)$. \square

S3 Generative Schemes under the Model

We describe below two generative schemes that can be thought of as generalizations of the IBP to our class of prior as well as to deal with non-binary scores. In particular, for the Bernoulli model this scheme is a straightforward consequence of Proposition 5 in [Camerlenghi et al. \(2022\)](#). For the Geometric model, it is a rewriting of Theorem S1.3.

S3.1 Bernoulli Model

1. In the first experiment day, $N_1 \sim \text{NegBin}(c + 1, 1 - \gamma_0^1 / (\beta + \gamma_0^1))$ users trigger.
2. After d -days suppose we have observed N_d unique users $\omega_1^*, \dots, \omega_{N_d}^*$, such that each user has triggered at least once a day for d_i days. Then on day $d + 1$, each of the previously seen user triggers independently of each other according to a Bernoulli distribution with parameter $(d_i - \alpha) / (d - \alpha + 1)$.

Moreover $N_{d+1}^* \sim \text{NegBin}(N_d + c + 1, 1 - \gamma_d^1 / (\beta + \gamma_0^{d+1}))$ new users (i.e., previously unseen) will trigger for the first time.

S3.2 Geometric Model

The triggering times for users active in the period $\{1, \dots, D^*\}$ is distributed as the random measure in Theorem S1.3, where we put $d = 0$ and $D^{up} = D^*$. In particular, the total number of users follows a Negative Binomial distribution with parameters $(c + 1, 1 - \gamma_0^{D^*}/(\beta + \gamma_0^{D^*}))$. The triggering times are i.i.d. random variables supported on $\{1, \dots, D^*\}$ such that

$$\Pr(Y_\ell = y) \propto B(1 - \alpha, y).$$

S4 Details on competing methods

To benchmark the performance of our newly proposed method, we consider a number of alternatives which have previously been proposed in the literature. We here provide additional details on these methods.

S4.1 Beta-binomial (BB) and beta-geometric (BG) predictors

The beta-binomial and beta-geometric models are (finite dimensional) Bayesian generative models for trigger data which work by imposing a pre-determined upper bound N_∞ on the number of units in the population, and assuming that for every unit $n = 1, \dots, N_\infty$ there exists a corresponding rate θ_n which governs the unit activity. In particular, these models assume

$$\theta_n \sim \text{Beta}(\alpha, \beta).$$

The beta-binomial model then assumes that we can observe for every day d of experimentation and every unit n where the unit triggered in the experiment on that day, and postulates

$$Z_{d,n} | \theta_1, \dots, \theta_{N_\infty} \sim \text{Bernoulli}(\theta_n),$$

i.i.d. across days d for the same unit n , and independently across different units. The beta-geometric model instead assumes that we can only observe for every unit n the “first trigger date” d_n , and postulates

$$Z_n | \theta_1, \dots, \theta_{N_\infty} \sim \text{Geometric}(\theta_n).$$

For the BB model, we use the estimator provided in [Ionita-Laza et al. \(2009, Section 1\)](#) to produce $U_{D_0}^{D_1}$. For the BG model, we adopt the Monte Carlo approach devised in [Richardson et al. \(2022, Section 3\)](#) to produce the corresponding estimates. We provide code to fit these models and produce the corresponding estimates.

S4.2 Jackknife (J) predictors

Jackknife estimators have a long history in the statistics literature, dating back to [Quenouille \(1956\)](#); [Tukey \(1958\)](#). Here we consider the jackknife estimators developed by [Gravel \(2014\)](#) who extended the work of [Burnham and Overton \(1979\)](#). In particular, the k -th order jackknife is obtained by considering the first k values of the resampling frequency spectrum; that is, by adequately weighting the number of users who appeared exactly $1, 2, \dots, k$ times in the experiment. We adapt the code provided in https://github.com/sgravel/capture_recapture/tree/master/software to form our predictions.

S4.3 Good-Toulmin (GT) predictors

Good-Toulmin estimators date back to the seminal work of [\(Good and Toulmin, 1956\)](#). Here, we adapt the recent approach of [Chakraborty et al. \(2019\)](#) for the problem of predicting the number of new genetic variants to be observed in future samples to online randomized experiments (in particular, we use the estimators provided in Equation (6) of the supplementary material). To form these predictions, we adapt to our setting the code provided in <https://github.com/c7rishi/variantprobs>.

S4.4 Linear programming predictors

Linear programs have been used for rare event occurrence ever since the seminal work of [Efron and Thisted \(1976\)](#). Here, we adapt to our setting the predictors proposed in [Zou et al. \(2016\)](#) via the `UnseenEST` algorithm. We adapt the implementation provided by the authors at <https://github.com/jameszou/unseenest> to perform our experiments.

S5 Additional Figures

Figure 9 shows the evaluation of the log-likelihood for an NB-SSP model.

Figure 11 reports the accuracy for the Be-SSP predictor on Zipf data for different choices of the tail parameter τ .

Figure 11 reports the accuracy for the total triggering activity of the NB-SSP predictor on proprietary data.

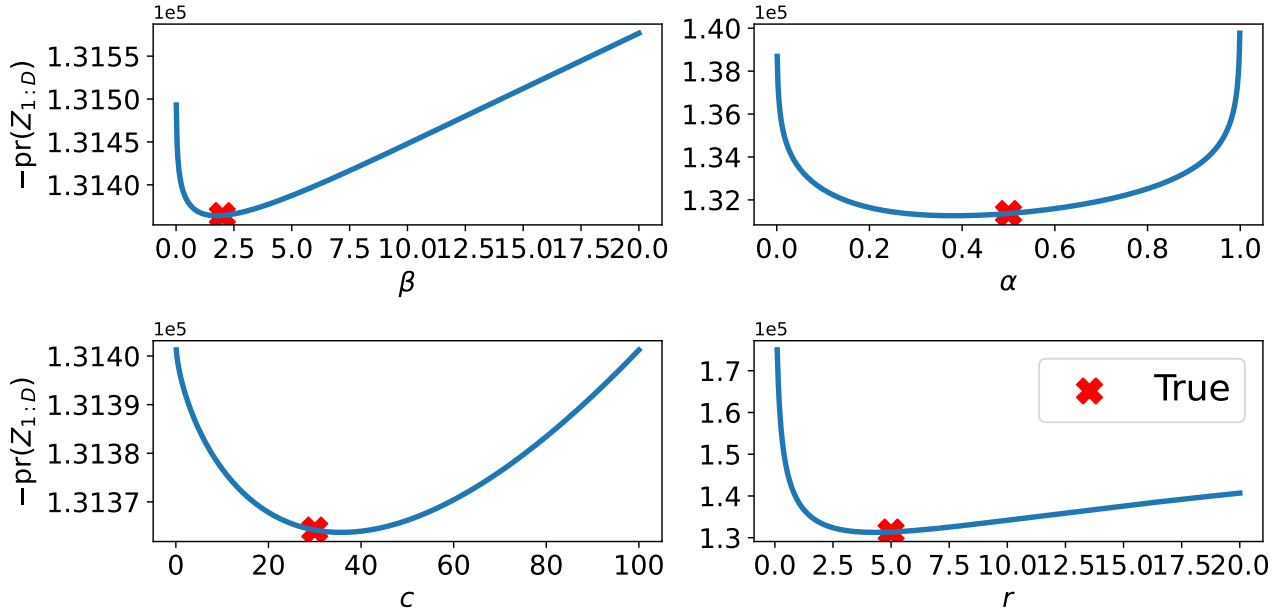


Figure 9: Evaluation of the log-likelihood in neighborhoods of the true values for data Z_1, \dots, Z_D from an NB-SSP model with $\alpha, \beta, c, r = (0.5, 2, 30, 5)$ and $D = 365$

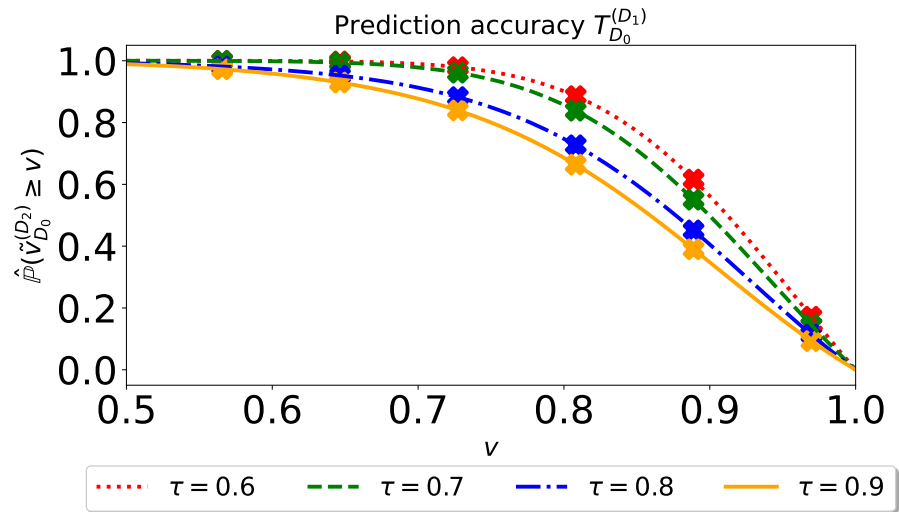


Figure 10: Prediction accuracy $\tilde{v}_{10}^{(50)}$ of the Be-SSP predictor on Zipf data for different choices of the parameter τ .

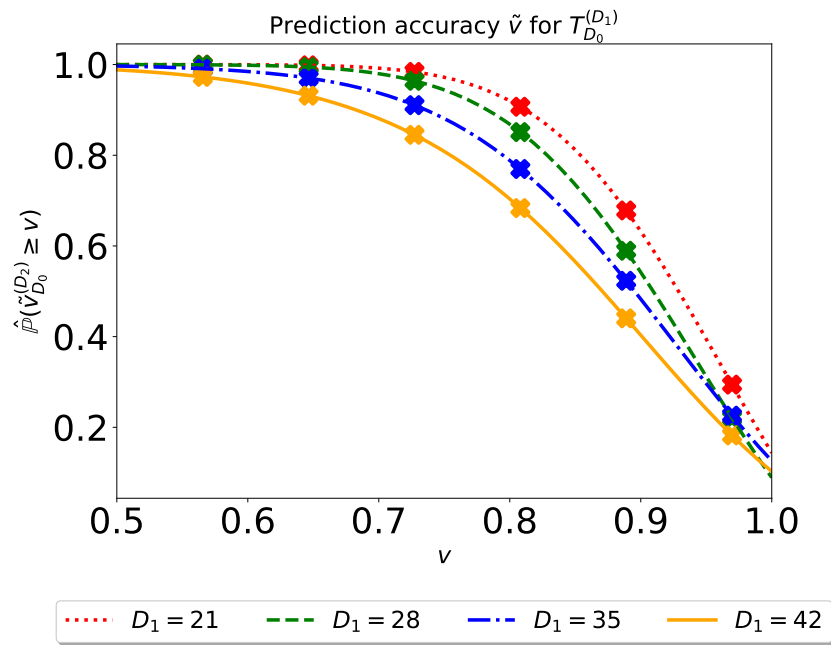


Figure 11: Survival plot for the prediction accuracy $\tilde{v}_{D_0}^{(D_1)}$ of the NB-SSP predictor for the total triggering activity (proprietary data). For a given accuracy level (horizontal axis), we plot the fraction of experiments achieving at least that level of accuracy (vertical axis) for different extrapolation values D_1 .